

Copyright
by
Chen Chia Lo
2013

The Report Committee for Chen Chia Lo
Certifies that this is the approved version of the following report:

Characteristics of Smoldering Combustion of Sawdust

APPROVED BY
SUPERVISING COMMITTEE:

Supervisor:

Janet L. Ellzey

Ofodike A. Ezekoye

Characteristics of Smoldering Combustion of Sawdust

by

Chen Chia Lo, B.S.M.E.

Report

Presented to the Faculty of the Graduate School of

The University of Texas at Austin

in Partial Fulfillment

of the Requirements

for the Degree of

Master of Science in Engineering

The University of Texas at Austin

May 2013

Dedication

I dedicate this paper to my parents for always being supportive and understanding in everything I do, and to my brother, for his humor and company.

Acknowledgements

I would like to thank my supervisor, Dr. Janet Ellzey, for her insightful guidance and support, Colin Smith and Erica Belmont for teaching me how to work the lab equipments and their endless patience, Brad Marvin for designing and building the chimney structure and assisting in experiments, Dr. Ofodike Ezekoye for his insights and comments on this paper, Home Depot and Berdoll Sawmill for providing the sawdust, and all the individuals who have worked on the Ghana project before me.

Abstract

Characteristics of Smoldering Combustion of Sawdust

Chen Chia Lo, M.S.E.

The University of Texas at Austin, 2013

Supervisor: Janet L. Ellzey

This report is a study on the smoldering combustion of natural sawdust from untreated woods. The objective was to develop and test an experimental technique to study the fundamental behavior of sawdust smolder. The experimental setup was an annulus cookstove packed with sawdust between the inner and outer radii creating a central hollow core. The sawdust was ignited by a heating coil wrapped around the inner radius. Thermocouples were embedded in the sawdust bed fanning out in the radial direction, and temperature was recorded throughout the smolder process. Consistent with the literature, the experimental results indicate that wood smolder consists of three pathways, 1) sawdust to char, 2) sawdust to volatiles, and 3) char to ash. Pathways 1 and 3 can be clearly characterized by the temperature profile of the smolder; however, pathway 2 often involves flaming of the sawdust and is beyond the scope of this study. Pathway 1, sawdust to char, is an endothermic reaction that results in a clearly defined char front that propagates across the sawdust bed in the radial direction. As smolder proceeds, the char continues to oxidize and breaks down into non-volatile products such as water vapor and carbon dioxide (CO₂) in further exothermic reactions. Pathway 2, char

to ash, is an exothermic reaction that can lead to glowing combustion when exposed to sufficient amounts of oxygen and results in spikes in temperature. In contrast to the clearly defined char front, the ashing zone traces cracks in the sawdust where air can penetrate through, and has no discernible front.

Section 1 discusses the motivation behind the study of sawdust cookstoves in third world countries, in particular Ghana, to replace wood with sawdust as a cheap alternative for household fuel. Section 2 details the experimental setup of the cookstove rig and the methodology of the experiments conducted. Section 3 reports the results of the experiments and analyzes the temperature profiles in relation to the three types of chemical reactions as noted above. Section 4 concludes with a summary of the results and discusses efforts in measuring emissions from the smolder and future work to be done.

Table of Contents

List of Tables	ix
List of Figures	x
Chapter 1: Biomass as Household Fuel Source in Third World Countries	1
1.1: Household Fuels in Third World Countries.....	1
1.2: Sawdust as the Fuel Source	2
Chapter 2: Background Information and Experiment Methodology	3
2.1: Biomass Combustion	3
2.2: Experiment Setup.....	4
Early Efforts at Ignition	6
Early Efforts at Emission Measurements.....	6
Repeatability	7
Chapter 3: Experimental Results	10
3.1: Types of Sawdust.....	10
3.2: Effect of Insulation	12
3.3: The Base Case.....	14
3.4: Effect of Air Flow.....	19
Chapter 4: Conclusions	22
Appendix A: Detailed drawings of the cookstove rig and the entry chamber	24
Appendix B: Test Case Conditions.....	26
Appendix C: Original Test Parameters	27
Appendix D: Smaller Diameter Cases	30
Appendix E: Base Case (2 and 4)	32
Appendix F: Base Case (3 and 3)	33
Appendix G: Base Case (3 and 3) with insulation.....	34
Appendix H: Air Flow Cases.....	36
Appendix I: Preliminary Emission Studies.....	38
References.....	40

List of Tables

Table B-1: Test case conditions	26
---------------------------------------	----

List of Figures

Figure 2-1: Assembly of sawdust cookstove rig.....	4
Figure 2-2: Thermocouple placements in the cookstove rig.....	5
Figure 2-3: Repeatability results for the first (outermost) thermocouple position	8
Figure 2-4: Repeatability results for the second thermocouple position	8
Figure 2-5: Repeatability results for the third thermocouple position.....	9
Figure 2-6: Repeatability results for the fourth (innermost) thermocouple position	9
Figure 3-1: Temperature profile of treated sawdust from Home Depot	11
Figure 3-2: Temperature profile of untreated sawdust from Berdoll Sawmill	11
Figure 3-3: Temperature profile of untreated sawdust burn without insulation around the cookstove	13
Figure 3-4: Temperature profile of untreated sawdust burn with insulation (ceramic fiber) around the cookstove	13
Figure 3-5: Temperature profile of the base case smolder burn	14
Figure 3-6: Thermocouple L4 profile on the primary ais divided into 5 main zones of temperature behavior	15
Figure 3-7: Webcam captures of the sawdust smolder process	17
Figure 3-8: Webcam captures comparing char to ash fronts	18
Figure 3-9: Example of glowing combustion	19
Figure 3-10: Base case smolder	20
Figure 3-11: Air flow rate at 0.16m/s	21
Figure A-1: Detailed dimensions of cookstove	24

Figure A-2: Detailed dimensions of entry chamber	25
Figure C-1: Original Case: No Flow, Test 1	27
Figure C-2: Original Case: No Flow, Test 2	27
Figure C-3: Original Case: 0.33m/s.....	28
Figure C-4: Original Case: 0.49m/s.....	29
Figure D-1: Smaller Diameter Case: No Flow, Test 2	30
Figure D-2: Smaller Diameter Case: No Flow, Test 3	30
Figure D-3: Smaller Diameter Case: 0.33m/s.....	31
Figure E-1: Base Case: No Flow	32
Figure F-1: Base Case: No Flow, Test 1	33
Figure G-1: Base Case: No Flow, with insulation, Test 2	34
Figure G-2: Base Case: No Flow, with insulation, Test 2	35
Figure H-1: Air Flow Case: 0.16m/s, with insulation, Test 1.....	36
Figure H-2: Air Flow Case: 0.16m/s, with insulation, Test 2.....	37
Figure I-1: GC measurements of CO and volatiles for a no air flow experiment...	38
Figure I-2: GC measurement of CO ₂ concentration in the exhaust	39

Chapter 1: Biomass as Household Fuel Source in Third World Countries

1.1 HOUSEHOLD FUELS IN THIRD WORLD COUNTRIES

The term Third World country was first used in the Cold War to refer to the countries that did not identify with the NATO member countries (First World) and the Common Bloc (Second World), but now is used interchangeably with developing countries and stereotyped to represent extremely poor countries with unstable economies. In developing countries, the struggle for accessibility of modern energy such as natural gas and petroleum is pervasive. According to Heltberg, the use of biomass fuels is “strongly inferior, declining with income” [1]. For both the urban poor and the rural countries, Ghana in particular, household fuel is heavily dependent on purchased firewood and kerosene, to the extent that “firewood has the highest budget share among its users” [1]. The implication is that the poorer households are the most exposed to firewood price fluctuations.

Unfortunately, in a study reported by Chronicle, Ghana suffers one of the highest rates of deforestation out of 65 nations, losing nearly 2.19% of its forest per year [2] while wood fuels amount to nearly 78% of all primary energy consumption source in the country [3]. The felled trees are generally used for charcoal, urban, or industrial feed stocks, with very small percentage accessible for household use. As the population grows rapidly, the demand for firewood multiplies in a similar fashion, quickly depleting the forest reserves in Ghana [2]. As the balance of wood fuel supply and demand shoots pass the break-even point, poorer families are faced with the difficulty of obtaining firewood at affordable price for household use. The situation mandates for affordable alternatives to substitute for and relieve the demand for wood fuels.

1.2 SAWDUST AS THE FUEL SOURCE

. Most developing countries invest the majority of their modern fuel source to industrial uses and are lacking in the appropriate infrastructures that improve energy accessibility for household use. When surveyed in a questionnaire, it is revealed that for households, fuel choice is more dependent on “availability when needed”, “availability near home”, or “ease of use when cooking” than the actual fuel price and cost of stove [4].

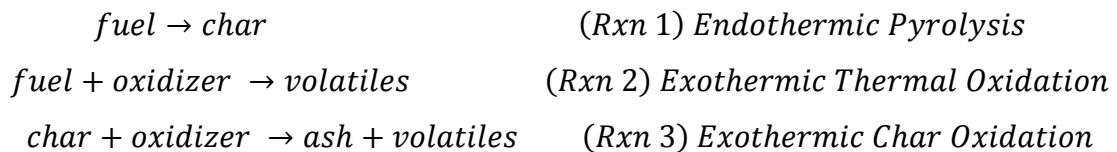
Sawdust has the potential to be a cheap alternative to wood fuel and is widely accessible and easy to use. It is a byproduct of the lumber industry and can be compressed into oven briquettes or packed tightly in a cookstove for household purposes. Extensive study must be done to determine the characteristics of sawdust combustion in comparison to wood fires to conclude whether sawdust is a viable substitute for wood fuel. These characteristics include flame temperatures, duration of burn, power output, and pollutant emissions. Studies in Accra, Ghana show that the household air pollution contains the highest particulate matter (PM) concentration in communities that use biomass fuels as the most common or even universal household fuel [4]. This is also motivation to study the emission of sawdust combustion in comparison to wood fires.

Chapter 2: Background Information and Experiment Methodology

2.1 BIOMASS COMBUSTION

Combustion processes require three key elements: fuel, oxidizer, and heat source. The heat source ignites the mixture of fuel and oxidizer, and the characteristics of the combustion process depend heavily on the ratio of fuel to oxidizer. Complete combustions yield products that consist of water vapor, carbon dioxide, and nitrogen, while incomplete combustions yield extraneous products such as carbon monoxide, nitrous oxide and nitrogen dioxide (NO_x), unburnt hydrocarbons (HC's) and particulate matters. Combustion of cellulosic materials generally falls into two regimes: flaming and smoldering. In the higher temperature regime, the fuel source breaks down into volatile combustible gases that induce flaming. In contrast, the second temperature regime produces water vapor, char and carbon dioxide much similar to a complete combustion process and occurs at a lower temperature [5]. The low temperature pathway is characterized by smoldering combustion and a clearly defined char front that propagates across the fuel bed, and produces ash as the char content continues to oxidize.

In Ohlemiller's study on modeling smoldering combustion propagation, he proposes that the process can be defined by three primary reactions pathways [6]:



The heat source provides the activation energy for the endothermic pyrolysis to convert the fuel to char and the exothermic thermal oxidation to produce volatiles. The energy generated by the exothermic process promotes char oxidization which forms ash

and combustible volatiles that can lead to a transition from smoldering to flaming combustion. Char smolder is extremely important to cookstoves due to its ability to sustain combustion up to six hours; this study will thus closely examine the temperature profile of the sawdust smolder to identify the reaction processes that are taking place.

2.2 EXPERIMENTAL SETUP

The cookstove used for the study is a design based on the sawdust cookstove described in Dahlman's and Forst's paper [7]. The rig is an aluminum annulus where the sawdust is tightly packed between the two diameters and is hollow in the center (Fig. 2-1). A heating coil is wrapped against the inner diameter of the saw dust bed to act as the ignition source. An entry chamber is attached to the bottom of the aluminum rig to create a uniform flow of air through the hollow center of the saw dust bed.

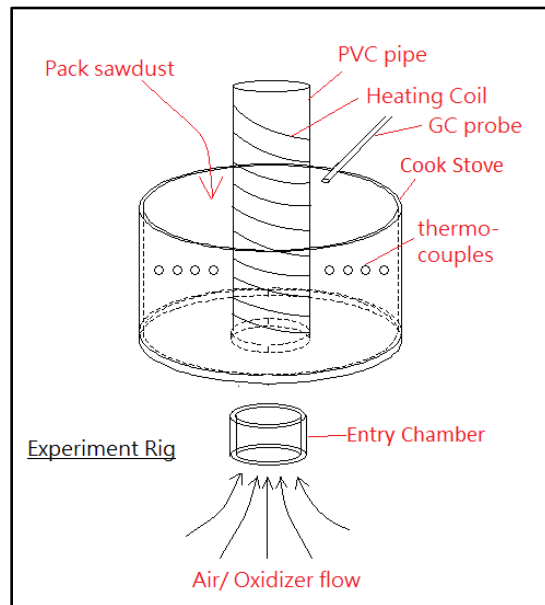


Figure 2-1. Assembly of sawdust cookstove rig.

The procedure for packing the saw dust bed is to first wrap the heating coil around the PVC pipe and fix it at the center of the annulus. The saw dust is then packed into the space between the PVC pipe and the wall of the annulus. After which, the PVC

pipe is carefully removed, leaving the heating coil behind, embedded against the inner radius of the saw dust bed. This creates the hollow center comparable to a chimney that allows the oxidizer to flow through.

The ignition of the saw dust bed is initiated by connecting the heating coil to a power supply for 10 minutes without any air flow. After ignition, the char front is allowed to propagate for 5 minutes before the mass controller is turned on and air is allowed to flow through the center of the bed.

The temperature profile is measured by two racks of Omega Type-E thermocouples with four thermocouples on each rack. The thermocouples are evenly distributed in the radial direction, and the height may be varied from 2 inches above the plate, to 3 inches and 4 inches (Fig. 2-2).

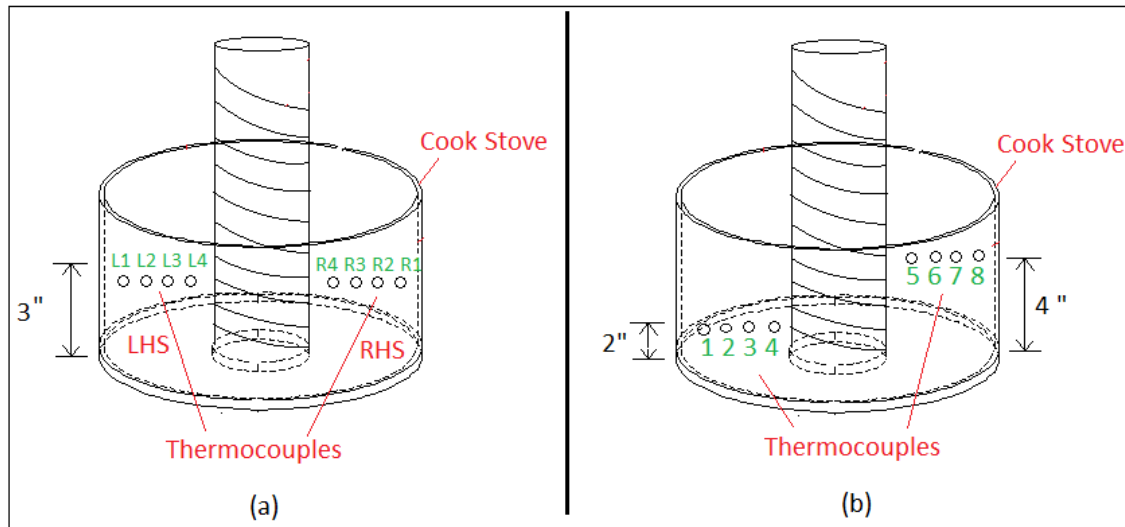


Figure 2-2. Thermocouple placements in the cookstove rig. For detailed dimensions of the cookstove, refer to Appendix A.

Early Efforts at Ignition

The current inner diameter is 1 inch, as opposed to the original 2.376 inches diameter in the early experimental setup. While attempting experiments that involve air flow, the smolder process often transitions to flaming combustion due to the increased ventilation of air throughout the sawdust bed. To resolve this problem, the inner diameter is shrunk to 1 inch and the air flow is only turned on after the smolder front has had some time to traverse into the sawdust bed. This allows the heat generated by the heating coil to be dissipated across a greater area to suppress transition to flaming combustion. This also increases the buffer distance between the heating coil and the innermost thermocouple so that the temperature observed at the location is mostly under the effect of the char front rather than the residual heat from the heating coil.

Early efforts also involved various trials at the delay time between turning off the heating coil and turning on the air flow. The goal is to turn on the air flow as soon as possible without incurring flaming combustion. For the air flow rate used in the final sets of experiments, a delay time of 10 minutes is sufficient to contain the flame to within the hollow core and eventually extinguish after about an hour. However, it is observed that higher flow rates tend to transition much more easily with very turbulent flames and may require a longer delay time.

Early Efforts at Emission Measurements

Initially, the emission was measured by a three channel gas chromatographer (GC) which reports concentration in mole fractions. The channels measure H_2 , N_2 , O_2 , CH_4 , CO , and various HC's. However, results from taking measurements at the char front and results from taking a series of measurements in one stationary location near the surface of the sawdust bed were inconclusive and may suggest that the GC needs to be calibrated to lower ppm ranges for the CH_4 , CO and HC's to attain results with improved accuracy.

The initial sets of experiments were conducted under open stove conditions, causing the emission measurements to be skewed by the surrounding air above the sawdust bed. At the time of writing, a chimney apparatus has been designed to fit onto the cookstove to redirect the exhaust flow and eliminate mixing with the ambient environment.

Repeatability

Ohlemiller [5] and others [12] have documented extensive research on cellulosic smolder combustion for wood; however, there are no temperature profiles for smoldering sawdust available in the literature. To validate the test results, repeatability tests were conducted for the base case to check for consistency. The base case conditions are: 1 inch inner diameter, no air flow, and thermocouple racks at 3 inches on the left and right hand sides of the rig. The results are plotted per thermocouple position in Figures 2-3 to 2-6. The two outermost thermocouples (Figs. 2-3 and 2-4) show up to 100°C in variation of peak temperature and a variation in the temporal location of the peak. These differences are most likely due to the irregular disintegration of the char body in the oxidation process. On the other hand, the two innermost thermocouples (Figs. 2-5 and 2-6) show greater consistency in both the magnitude and location of the peak temperature.

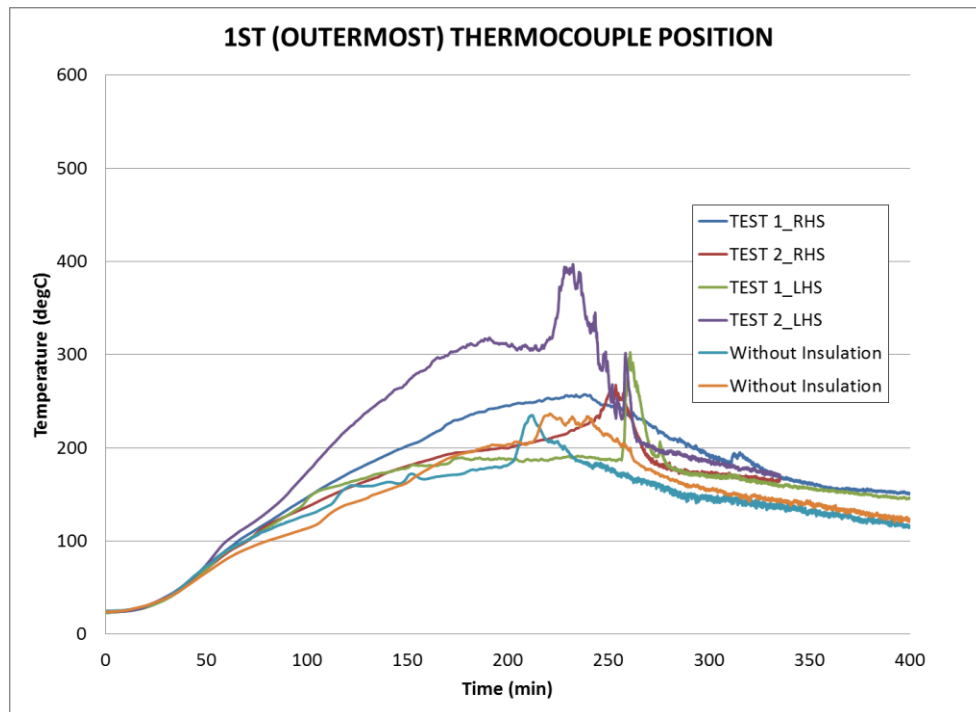


Figure 2-3. Repeatability results for the first (outermost) thermocouple position. Spikes are due to char residues on the thermocouple bead (see Section 3.3).

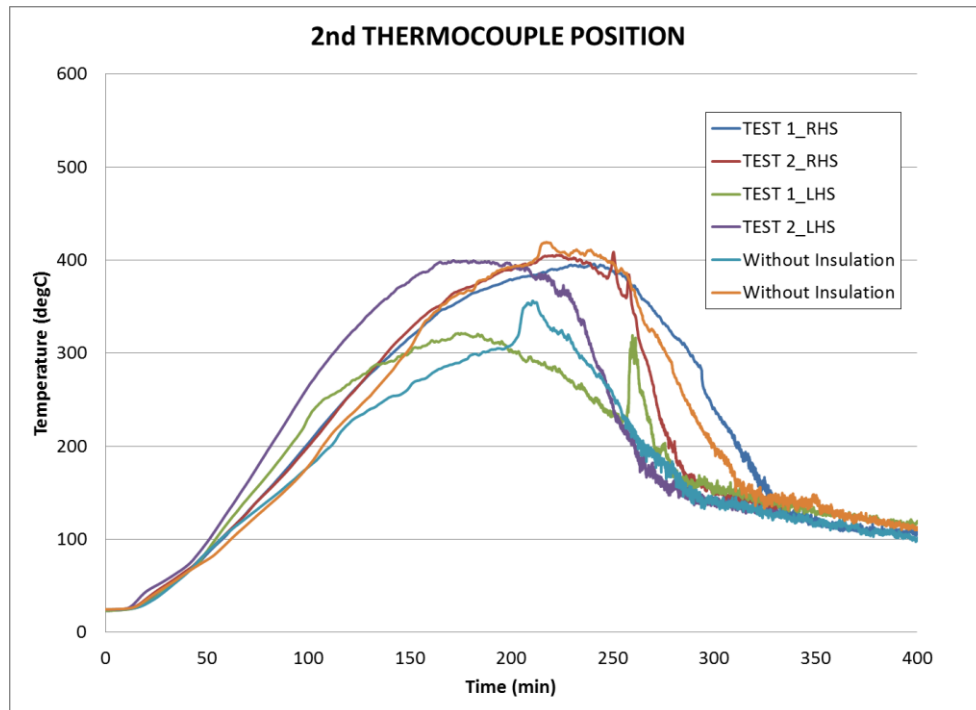


Figure 2-4. Repeatability results for the second thermocouple position.

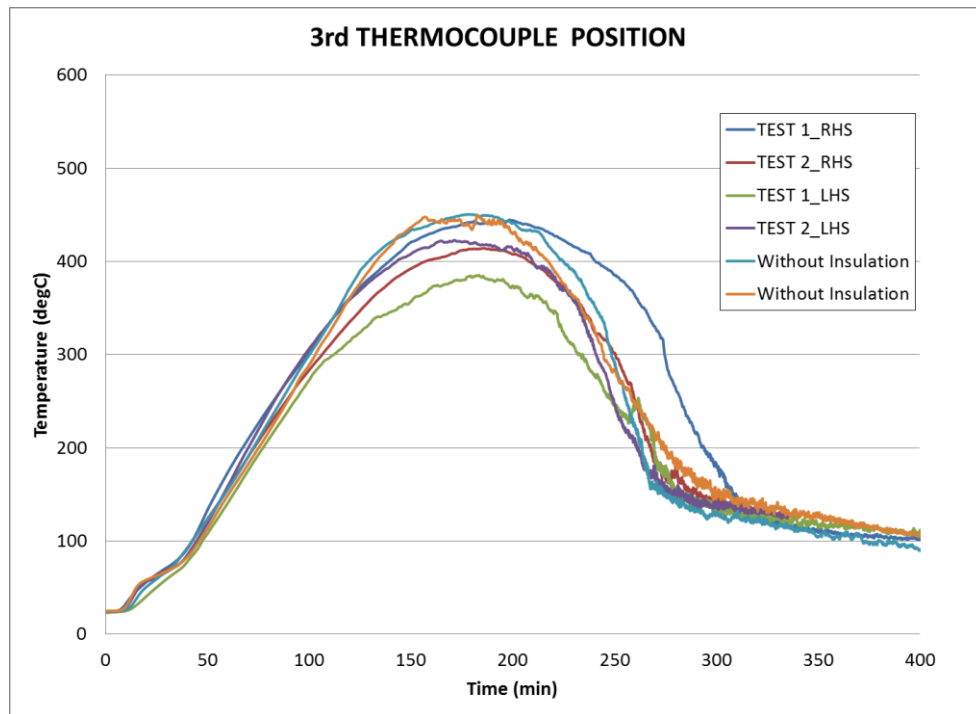


Figure 2-5. Repeatability results for the third thermocouple position.

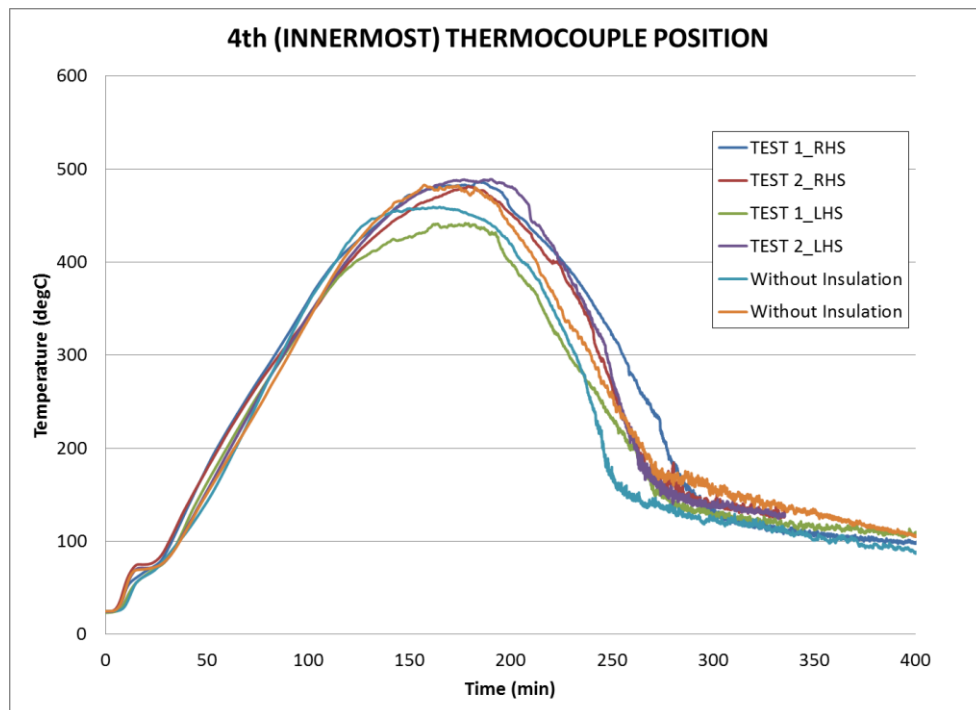


Figure 2-6. Repeatability results for the fourth (innermost) thermocouple position.

Chapter 3: Experimental Results

3.1 TYPES OF SAWDUST

During the course of developing the experiment, the two main sources of sawdust were Home Depot, where the sawdust is mostly chemically treated pine wood, and Berdoll Sawmill, where the sawdust is mostly untreated mesquite. Figures 3-1 and 3-2 are the thermocouple results of sawdust smolders with no air flow through the center core, and measured at a height of 4 inches above the base of the rig. The results show that the maximum temperatures during the burns are very similar (approximately 400°C for both types of sawdust), and the initial smolder behavior up to $t = 150$ minutes are comparable as well. In the first 10 minutes, there is the initial temperature rise due to the heating coil. Then the temperature profile flattens out for 30 to 50 minutes until it takes off again. Before reaching the peak temperature, the temperature rise can be divided into two zones: one which increases at a steep temperature rise, and the next which seems to flatten out again until the peak temperature. After the smolder reaches peak temperature, the profile steadily cools off with occasional spikes in temperature.

Although Figure 3-1 suggests that the Home Depot sawdust has a slightly longer cooling period than the untreated sawdust, the smolder behavior between the two is similar enough to suggest that the fundamental processes are likewise similar. The temperature spikes in Figure 3-1 are due to char remnants residing on the thermocouple that nearly transition to flaming combustion before flaking away, and are thus irrelevant to comparing the smolder behaviors. This will be discussed in more details in following sections.

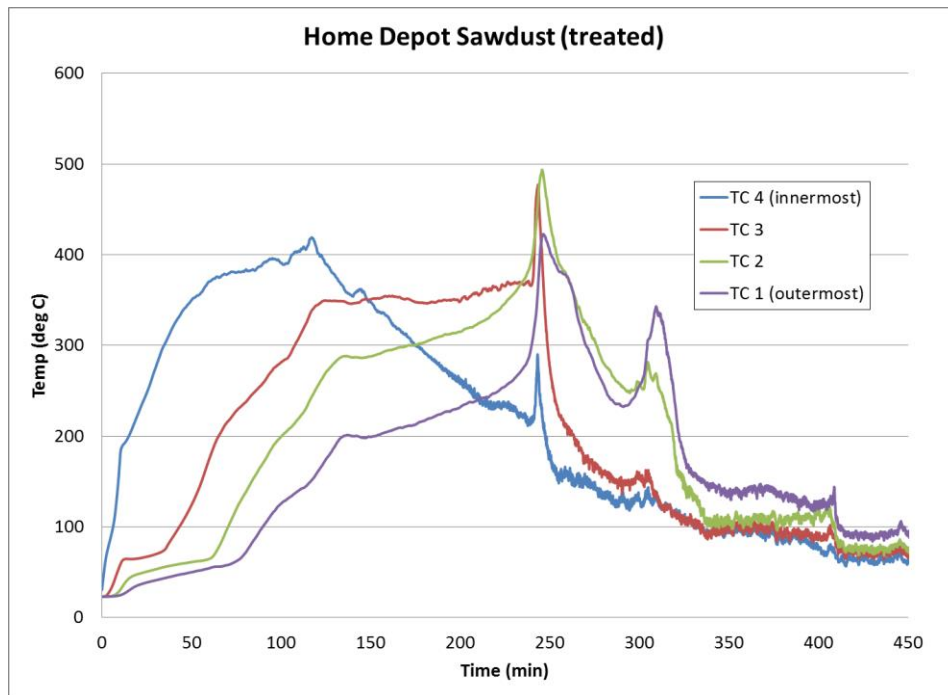


Figure 3-1. Temperature profile of treated sawdust from Home Depot. No flow, 4 inches above base of rig.

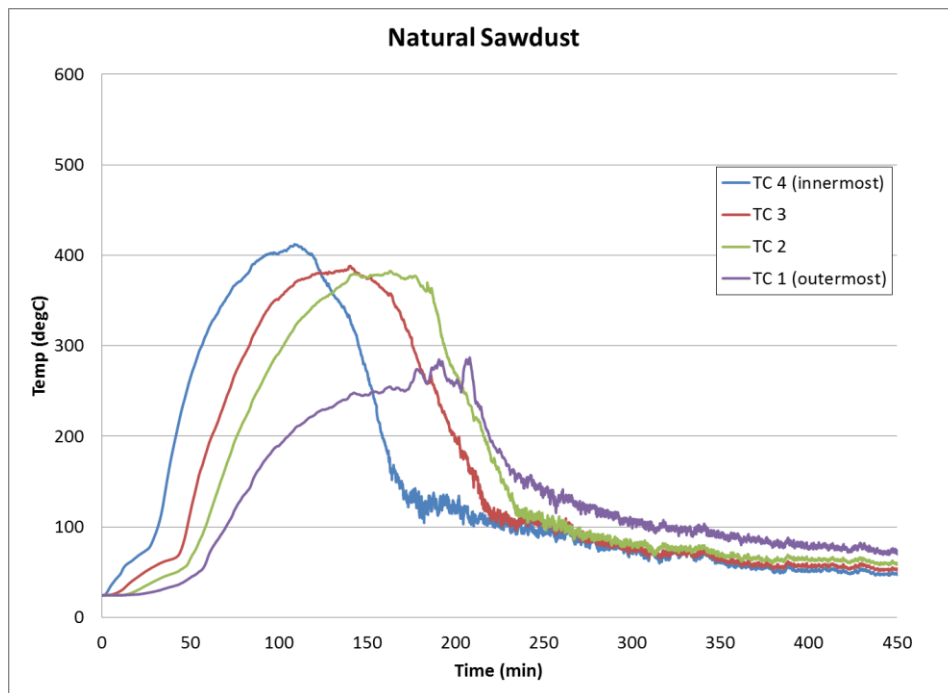


Figure 3-2. Temperature profile of untreated sawdust from Berdoll Sawmill. No flow, 4 inches above base of rig.

3.2 EFFECT OF INSULATION

The experimental cookstove is modeled after a sawdust cookstove designed in Dr. Ellzey's lab by Alex Breckel and Rahul Jain, and is made of an aluminum pipe with thickness of 0.25 inches. While sawdust can be effective insulation and would eliminate the need for insulation around the cookstove wall, it is important to check that this assumption is valid. Figures 3-3 and 3-4 are results for sawdust burns with no flow through the center core and thermocouples measuring at 3 inches above the base of the rig.

The results show that the peak temperatures and the transient behaviors of the smolders with or without insulation are extremely similar and that heat loss from the cookstove wall does not significantly affect the results. This supports that the sawdust bed acts as both the fuel and the insulation for the cookstove.

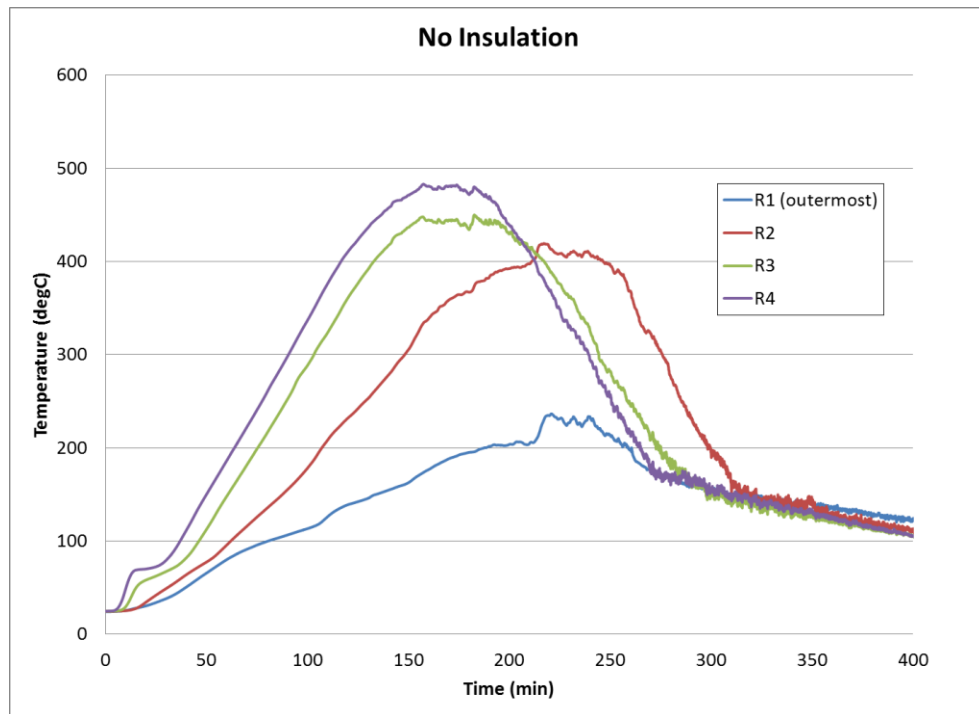


Figure 3-3. Temperature profile of untreated sawdust burn without insulation around the cookstove. No flow, 3 inches above base of rig.

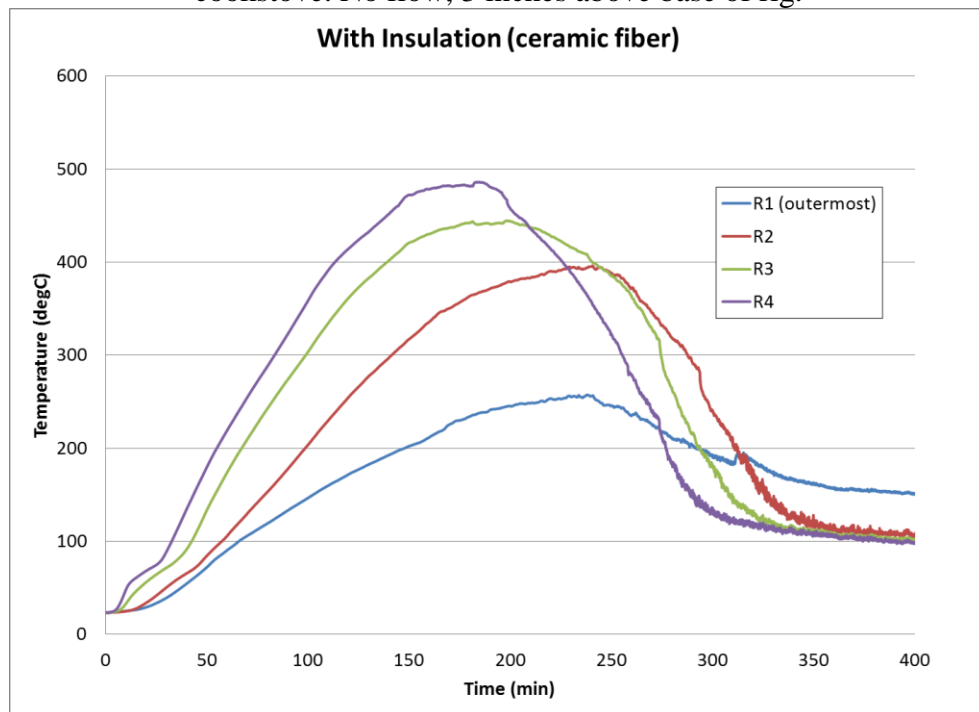


Figure 3-4. Temperature profile of untreated sawdust burn with insulation (ceramic fiber) around the cookstove. No flow, 3 inches above base of rig.

3.3 THE BASE CASE

In this section, the base case will be discussed in detail to explain the temperature profile in relation to the reactions taking place. The base case test conditions are: no air flow, both thermocouple racks at 3 inches above the base of the cookstove rig, untreated mesquite sawdust, and inner diameter of 1 inch. Figure 3-5 is a representative temperature profile for the base case. Refer to Appendix B for other smolder test conditions that were performed.

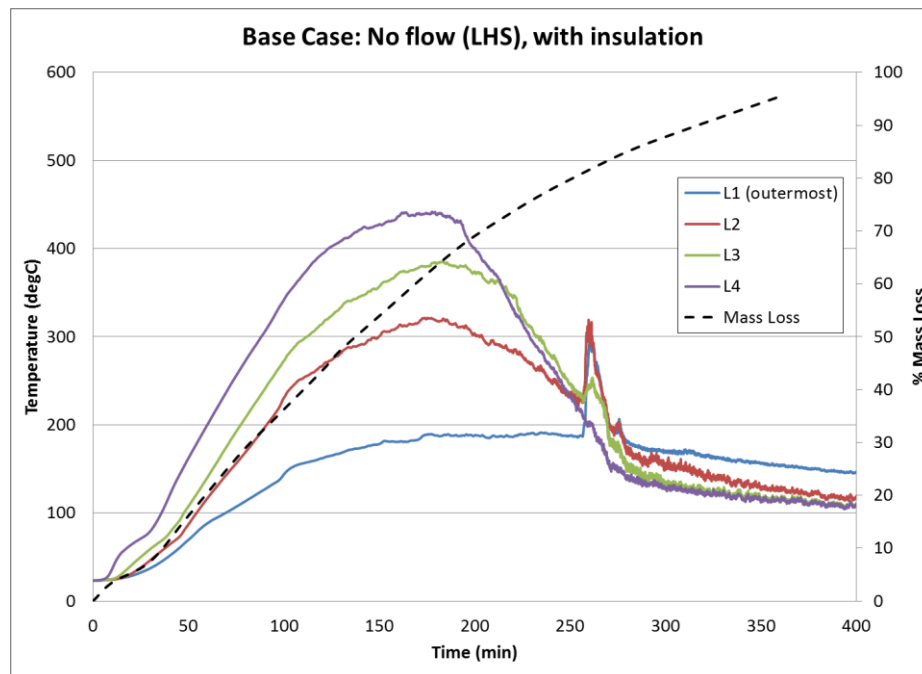


Figure 3-5. Temperature profile of the base case smolder burn on the primary axis (to the left). No flow, 3 inches above base of rig, left-hand side thermocouple rack. Mass loss % of the fuel bed on the secondary axis (to the right).

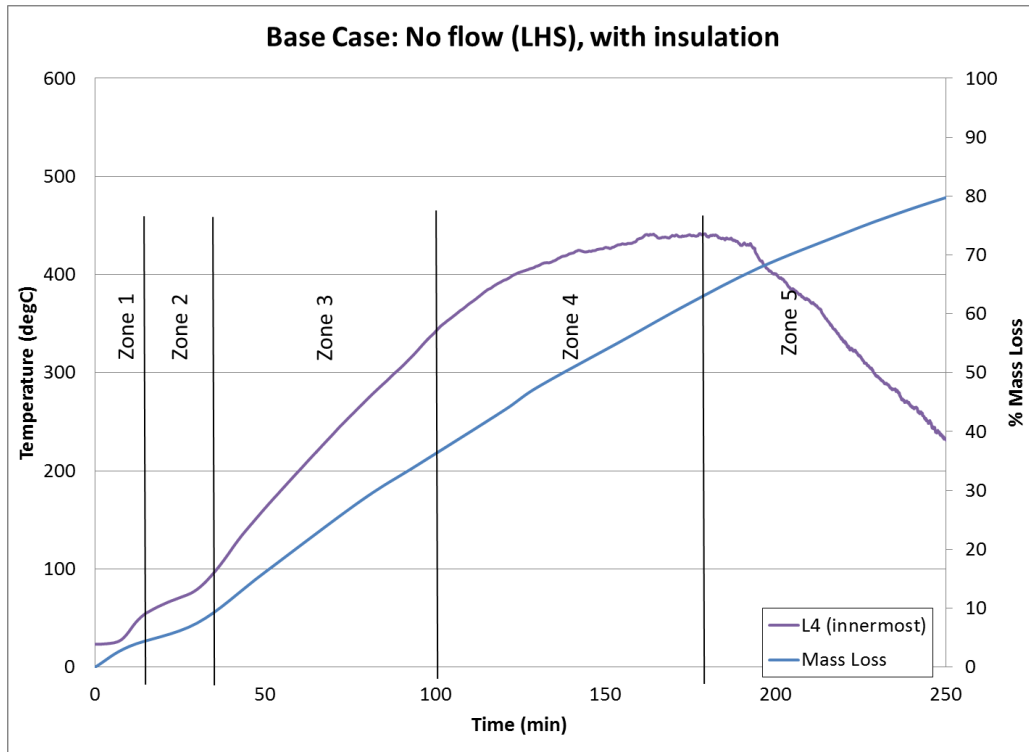


Figure 3-6. Thermocouple L4 profile on the primary axis (to the left) divided into 5 main zones of temperature behavior. Mass loss % of the fuel bed on the secondary axis (to the right). Corresponding webcam captures during the smolder can be seen in Figure 3-7.

The smolder behavior can be roughly divided into 5 main stages for each thermocouple. First, the temperature takes off quickly due to the heating coil (Zone 1); then the temperature flattens out (Zone 2). Next the temperature takes off quickly again (Zone 3), followed by another plateau until the temperature profile reaches its peak (Zone 4). After which, the temperature cools off steadily with occasional spikes in temperature (Zone 5). Figure 3-6 marks the boundaries of the five zones.

In Zone 1, the temperature rises due to conduction heat transfer from the heating coil. During this period, the sawdust bed absorbs the thermal energy to pyrolyze the fuel until the char front begins to form in Zone 2 (Fig. 3-7 b).

Zone 2 is a competition for fuel between reaction 1 (exothermic conversion of fuel/air to volatiles) and reaction 2 (endothermic conversion of fuel to char). As suggested by Ohlemiller [6], the reaction of fuel and oxidizer is an exothermic process which produces volatiles, and can lead to the transition from smolder to flaming. In some cases, flaming transition was observed in the experiments with air flow. The increased flow rate of oxidizer enhances the exothermic reaction and produces more volatiles, thus increasing the rig's susceptibility to transition. On the other hand, the reaction pathway from fuel to char is an endothermic pyrolysis, and accounts for the main reason that the temperature profile flattens out. Figure 3-7 (b) to (f) shows the process in Zone 2 where the char front propagates from the inner diameter to the outer edge of the fuel bed and pyrolyzed most of the sawdust into char. Although there is no forced air flow in the base case, a chimney draft forms in the hollow core of the sawdust bed. As the sawdust undergoes pyrolysis and turns into char, the density of the fuel bed becomes more porous and allows for better ventilation of oxidizer through the fuel bed. The enhanced distribution of air due to the porous nature of char and ash can be interpreted from Figure 3-6, which shows the percent of mass loss over time on the secondary axis. The mass of the fuel bed is measured at various intervals during the smolder process for a no flow base case. The figure shows that by the end of the combustion process, the fuel bed has lost more than 80% of its original mass and yet still retains a significant portion of its volume, as indicated in Figure 3-7 (k). This is strong indication that the fuel bed loses a substantial amount of density during the smolder and allows for air to flow through the fuel bed and oxidize the char.

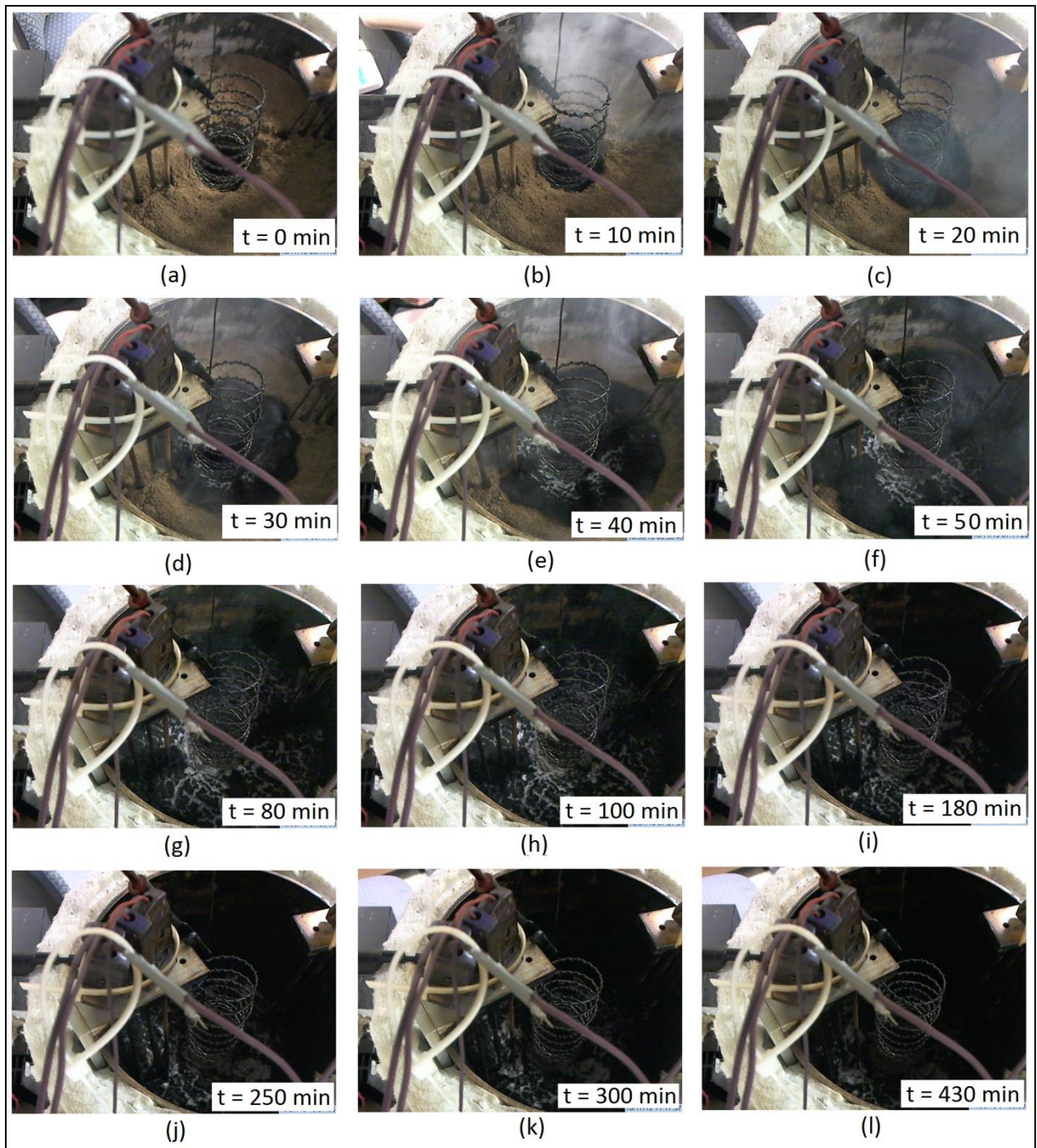


Figure 3-7 (a) to (l). Webcam captures of the sawdust smolder process.

In Zone 3, the char front has completely propagated to the rig wall, and the overall composition of the fuel bed consists of some unburnt sawdust and mostly pyrolyzed char. The dominating reaction pathway is the exothermic reaction of char and oxidizer to form ash and volatiles. This leads to the temperature increase in Zone 3. Unlike the charring pathway, there is no discernible front for ashing; rather it occurs along cracks in the fuel bed where air is able to flow. Figure 3-8 shows a comparison between the clearly defined char front (a) versus the char oxidation regime which is visible by the grey areas in (b).



Figure 3-8. Webcam captures comparing char to ash fronts.

In Zone 4, all of the sawdust is pyrolyzed and the process is completely dominated by the exothermic char oxidation pathway to form combustion products such as water vapor, CO_2 , N_2 , ash, and some volatiles. However, while thermal energy is generated by char oxidation, the enhanced air ventilation incurs significant heat loss through convection at the same time. Thus the reaction process continues until there is not enough thermal energy to oxidize the remaining char. The peak temperature occurs only because the sawdust bed is shrinking and losing its mass throughout the smolder process until eventually the thermocouples are exposed to the ambient environment and experience significant convective heat loss. Therefore, even though Zone 5 is a different temperature behavior than Zone 4, the dominating reaction is still the same, only that the

thermocouples are no longer embedded within the bed. If the experiment is setup so that the thermocouple remains embedded within the fuel bed all throughout the smolder process until the ash stops oxidizing, it is likely that the temperature would be able to reach its true peak, higher than the observed peak temperature.

As mentioned before, the temperature profile occasionally captures a sharp spike during the char oxidation process. This is due to the formation of volatiles. By the nature of smolder, remnants of char sometimes reside on the thermocouple bead. When exposed to high air flow rate, the remnant can either cool off quickly or oxidize to form volatiles that begin to transition to flaming combustion (Fig. 3-9). However, usually there is not enough thermal energy for the residue to transition completely before it flakes away.



Figure 3-9. Example of glowing combustion. The red circle marks a spot where the char is transitioning to flaming, as shown by the glowing combustion.

3.4 EFFECT OF AIR FLOW

In a practical cookstove, the flow of air is controlled by a vent and is an important parameter for controlling the combustion and smoldering processes. In this study, the base case with no forced air flow (Fig. 3-10) is compared to a case with a flow velocity of 0.16m/s air flow (Fig. 3-11). These results show that the peak temperature for each

thermocouple for the case with air flow is higher by about 50 °C to 100°C. The increase in peak temperature occurs due to enhanced reaction rate of the exothermic pathway in the fuel bed. This enhancement can often lead to transition to flaming combustion.

Comparing Figures 3-10 and 3-11, the transition between Zone 3 and Zone 4 is more gradual in the 0.16m/s case, and the boundary between the two zones almost cannot be distinguished. This is possibly due to the air flow facilitating the convective cooling process, distributing the air more evenly across the entire fuel bed. However, the overall combustion process for either of the two cases are complete within 300 minutes and suggests that air flow does not seem to have a significant effect on the combustion rate of the smolder. It is likely that the tested air flow rate is not high enough to cause an identifiable change in the combustion rate.

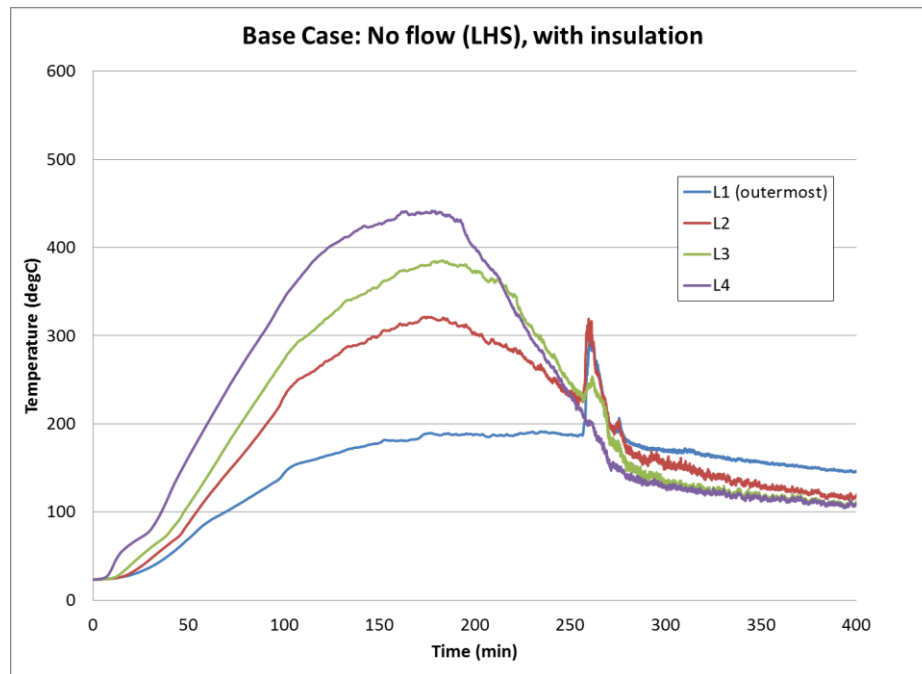


Figure 3-10. Base case smolder. No flow, 3 inches above base of rig.

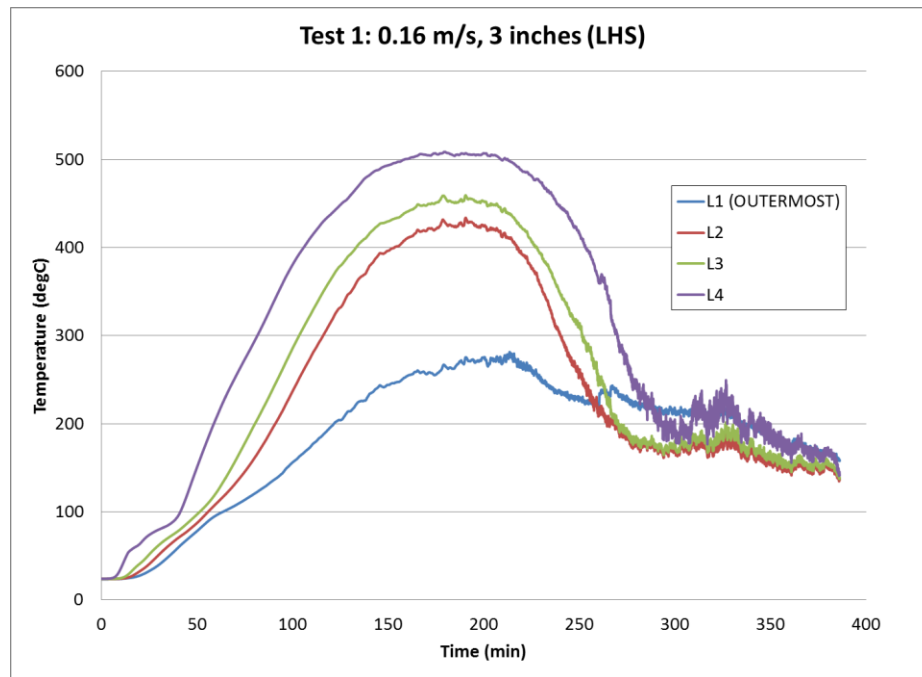


Figure 3-11. Air flow rate at 0.16m/s, 3 inches above base of rig.

Chapter 4: Conclusions

The goal of this prototypal study was to develop an experimental technique that would lead to an elementary understanding of the smolder of sawdust. The results show that for the purposes of this study, the type of sawdust (treated or untreated, pine or mesquite) has little effect on the temperature profile of the combustion and on smolder trends. Experiments also show that since sawdust is commonly used as a household insulator, the cookstove does not experience significant heat loss and does not need to be insulated.

The base case results are helpful to observe the three main reaction pathways that take place during a smoldering combustion. First, there is the fuel to char, endothermic pyrolysis that can be identified as the char front. Then there is the exothermic process that oxidizes the fuel and air mixture to produce ash and volatiles. This process generates significant amounts of heat and can sometimes lead to glowing combustion or transition to flaming combustion depending on the air flow rate. Finally, the last reaction pathway is the exothermic oxidation of char to produce combustion products such as water vapor, CO₂, N₂, ash and more volatiles. This is when the combustion process reaches its peak temperature and begins to cool down until there is not sufficient thermal energy to further oxidize the remaining char. Occasionally, the volatiles react with the air flow and leads to glowing combustion, but there is not enough energy for the volatile to transition to flaming combustion.

Future Work

The results are only preliminary studies on the smoldering combustion of sawdust; more work still has to be done to determine the feasibility of replacing wood fuels in low-income households and the optimal design of the cookstove to maximize sawdust as the fuel source. The next step is to record the CO and unburnt HC emissions

during the smolder processes as well as measure the concentration of particulate matter. It would be useful to observe how changing the air flow rate or the air-fuel ratio can impact the concentration of the emissions and how that compares to emissions when burning wood logs. Some preliminary work has already been done for emission measurements (Appendix I); however these are measured in open stove conditions where the ambient environment may have significant impact on the readings. At the time of writing this report, a chimney structure has been built with the help of undergraduate research assistant, Brad Marvin, to direct the exhaust flow and take emission measurements in the chimney where the sample is completely from the smolder process.

Future work can also be done to change the geometry of the cookstove to enhance the smolder rate of the sawdust or to determine the boundaries of transition from smolder to flames.

Appendix A: Detailed Drawings of the cookstove rig and the entry chamber

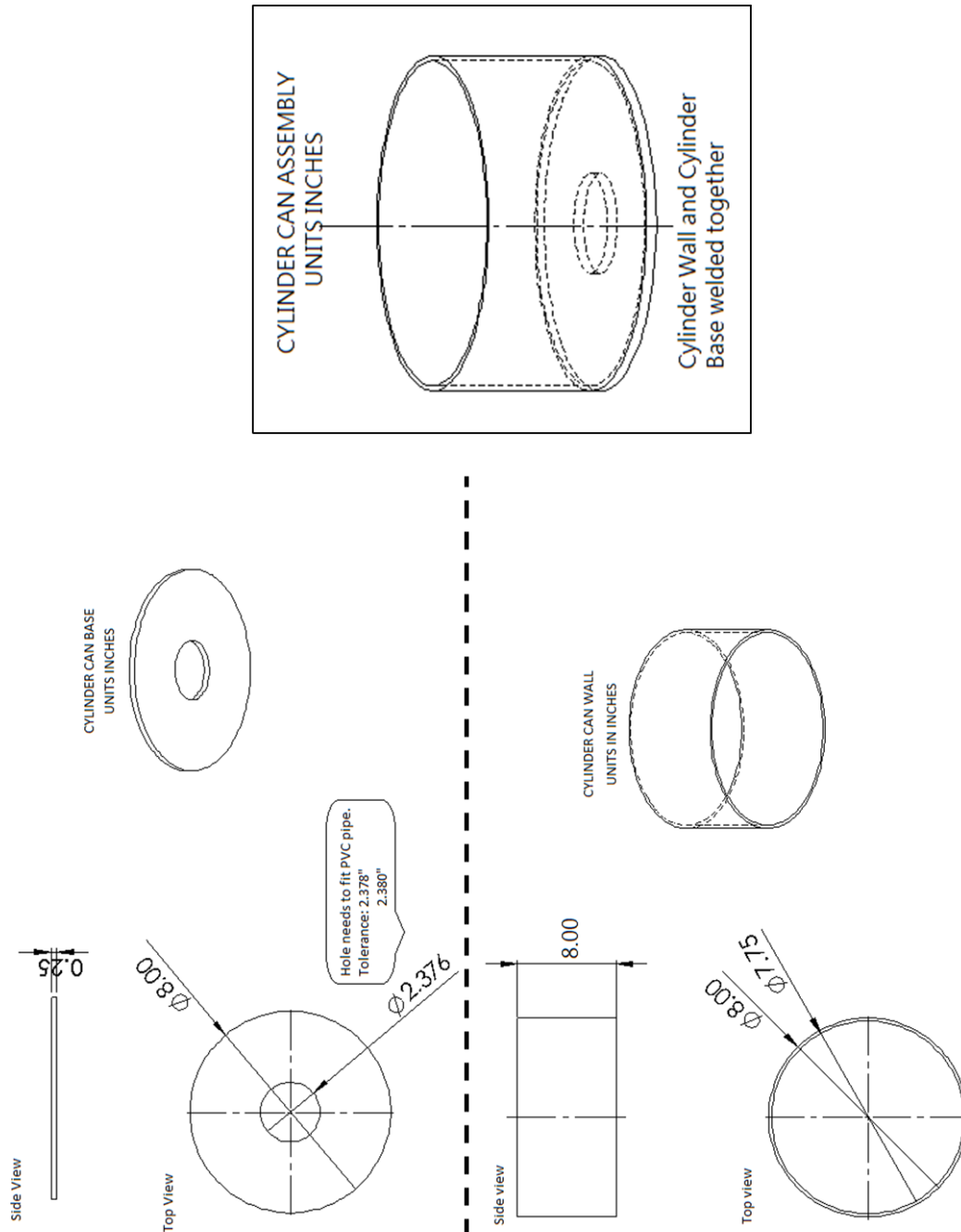


Figure A-1. Detailed dimensions of cookstove.

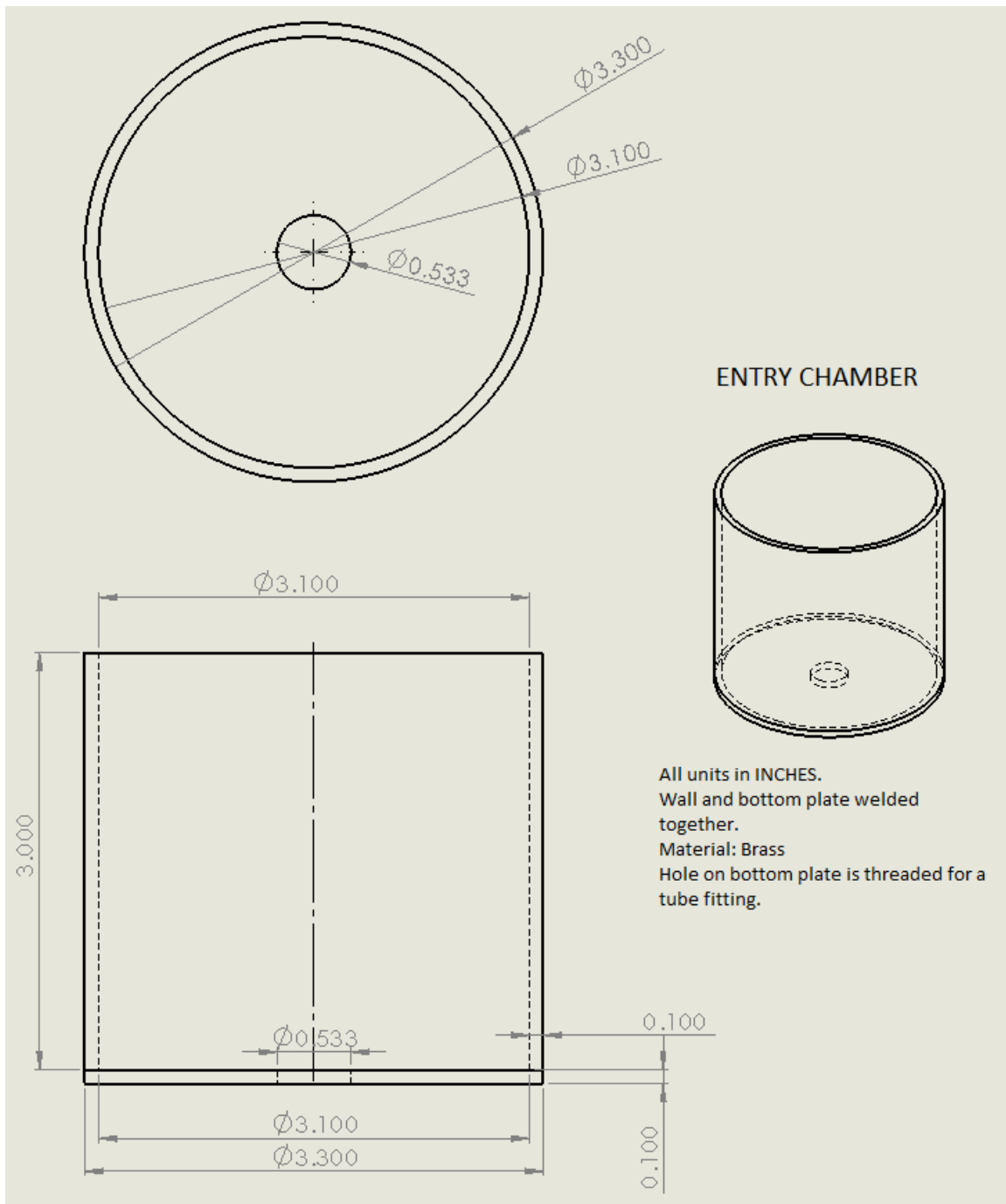


Figure A-2. Detailed dimensions of entry chamber.

Appendix B: Test Case Conditions

Table B-1. Test case conditions

	Sawdust Type	Air Flow Rate (m/s)	Inner Diameter (inch)	Insulation (Y/N)	Thermocouple height above base of rig (inch)	Comments	Experimental Results
Original Case	Treated Pine	0	2.376	N	2 and 4	Some thermocouples were incorrectly calibrated.	Appendix C
	Treated Pine	0.33	2.376	N	2 and 4		
	Treated Pine	0.49	2.376	N	2 and 4		
Small D	Treated Pine	0	1	N	2 and 4		Appendix D
	Treated Pine	0.33	1	N	2 and 4		
Base Case (2,4)	Untreated Mesquite	0	1	N	2 and 4		Appendix E
Base Case (3)	Untreated Mesquite	0	1	N	3 and 3		Appendix F
Base Case (3)	Untreated Mesquite	0	1	Y	3 and 3	Discussed in detailed in 3.3	Appendix G
Air Flow	Untreated Mesquite	0.4	1	Y	3 and 3	Discussed in detail in Section 3.4	Appendix H

Appendix C: Original Test Parameters

Note: Some of the thermocouples were not calibrated correctly and the resulting erroneous data are omitted.

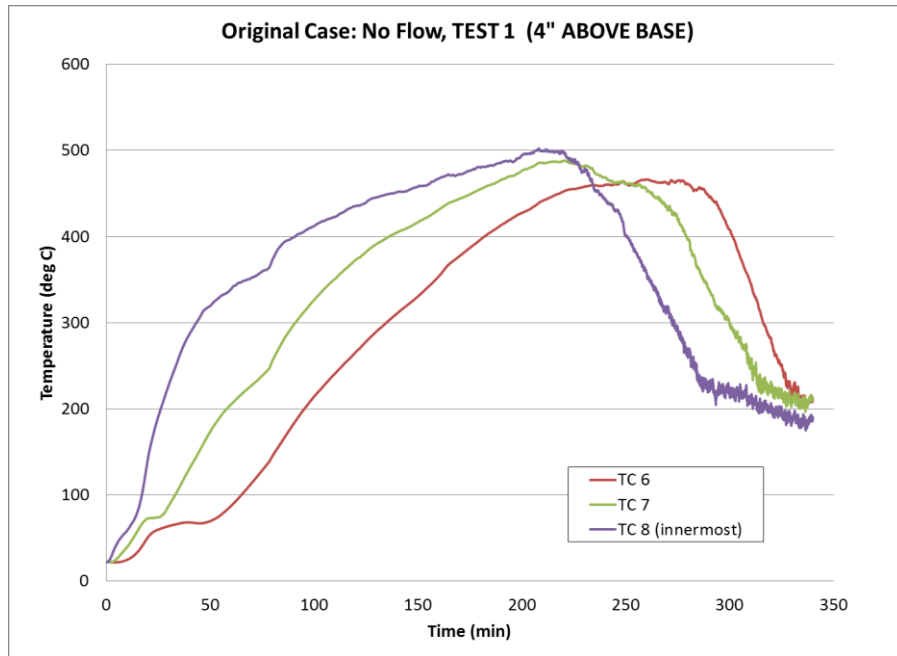


Figure C-1. Original Case: No Flow, Test 1.

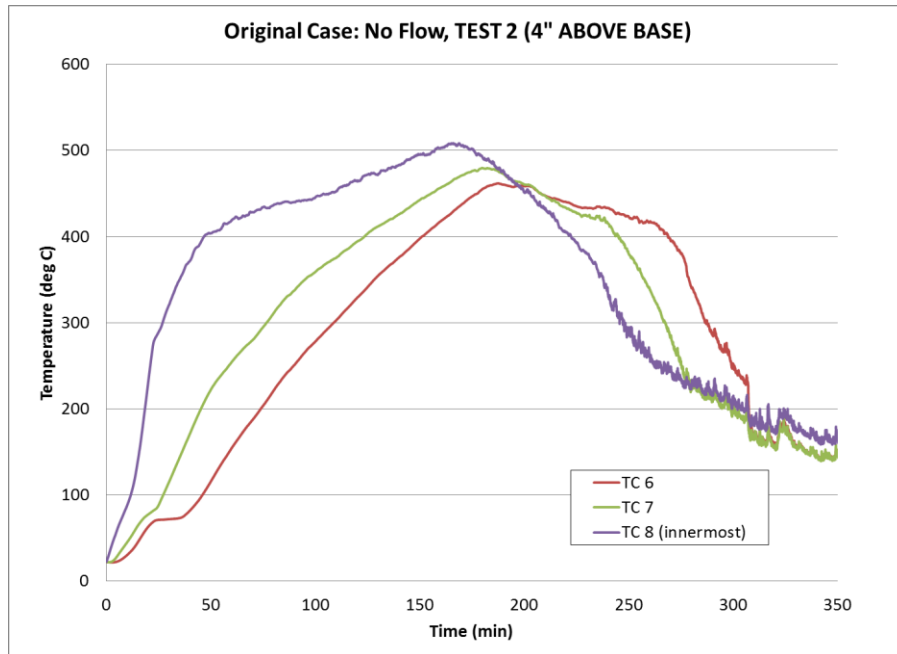


Figure C-2. Original Case: No Flow, Test 2.

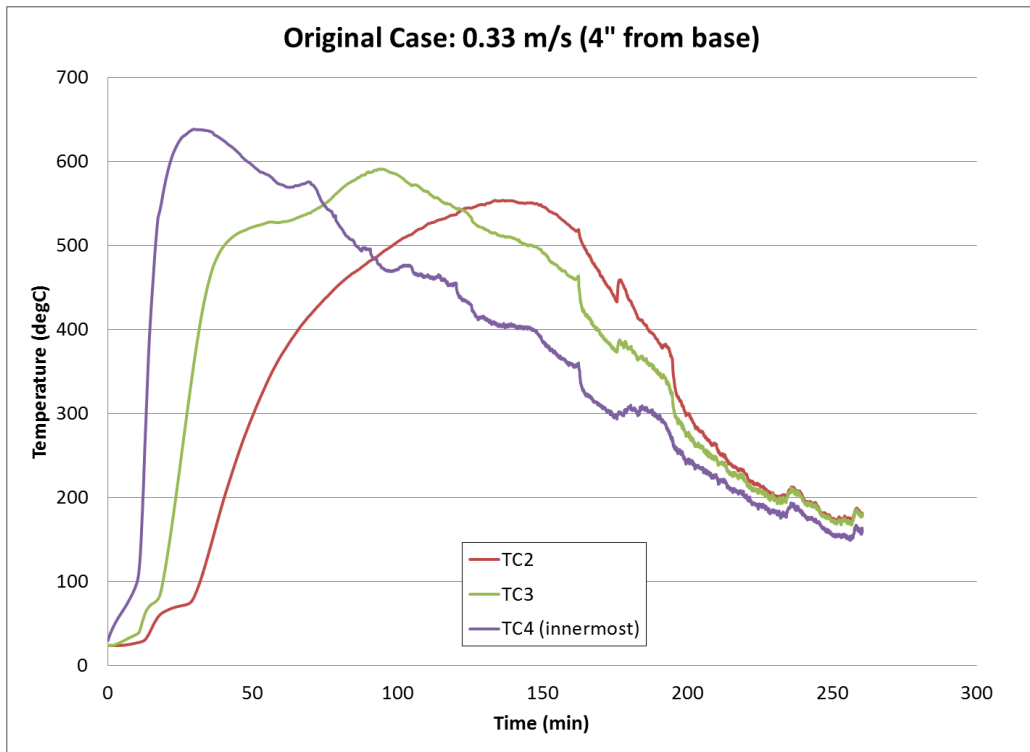
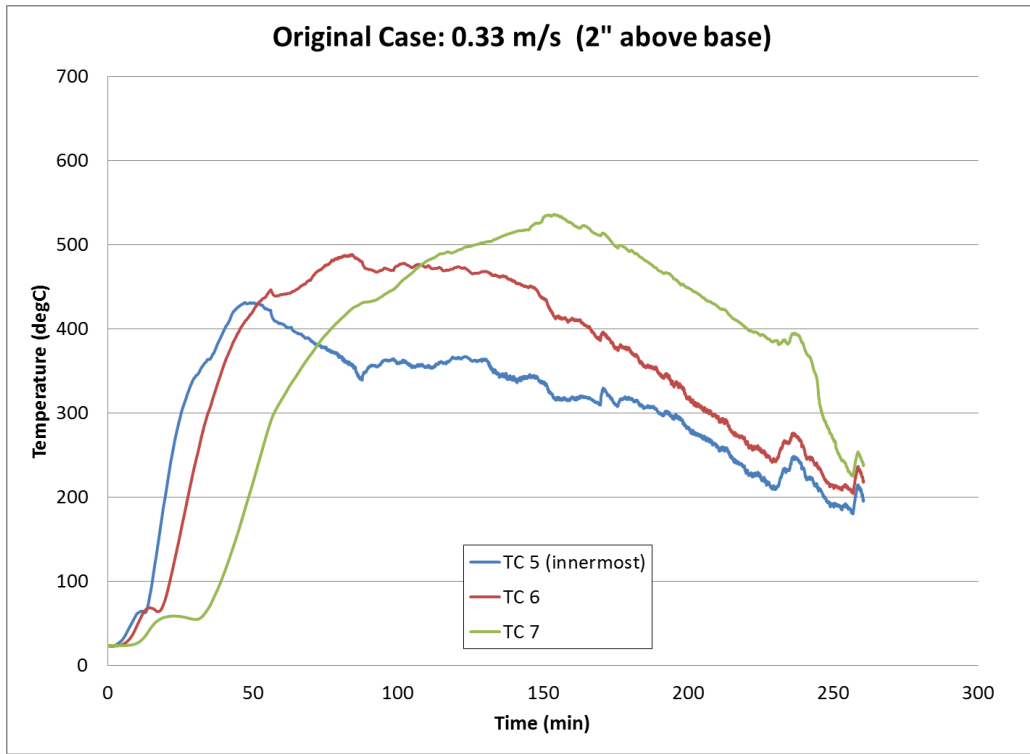


Figure C-3. Original Case: 0.33m/s.

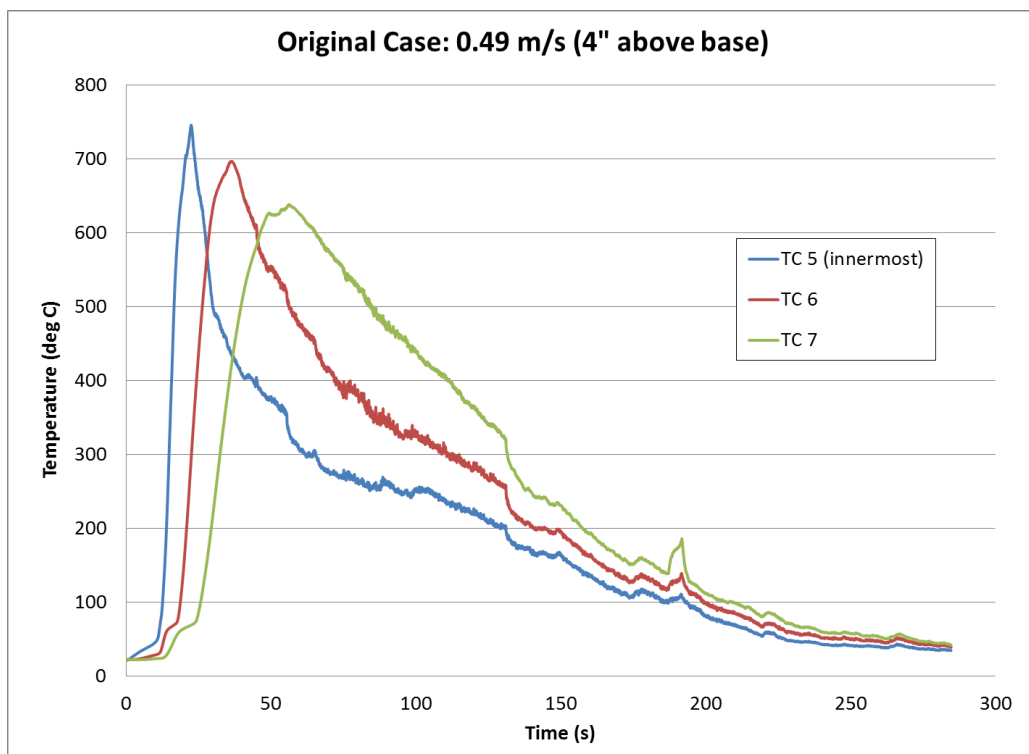
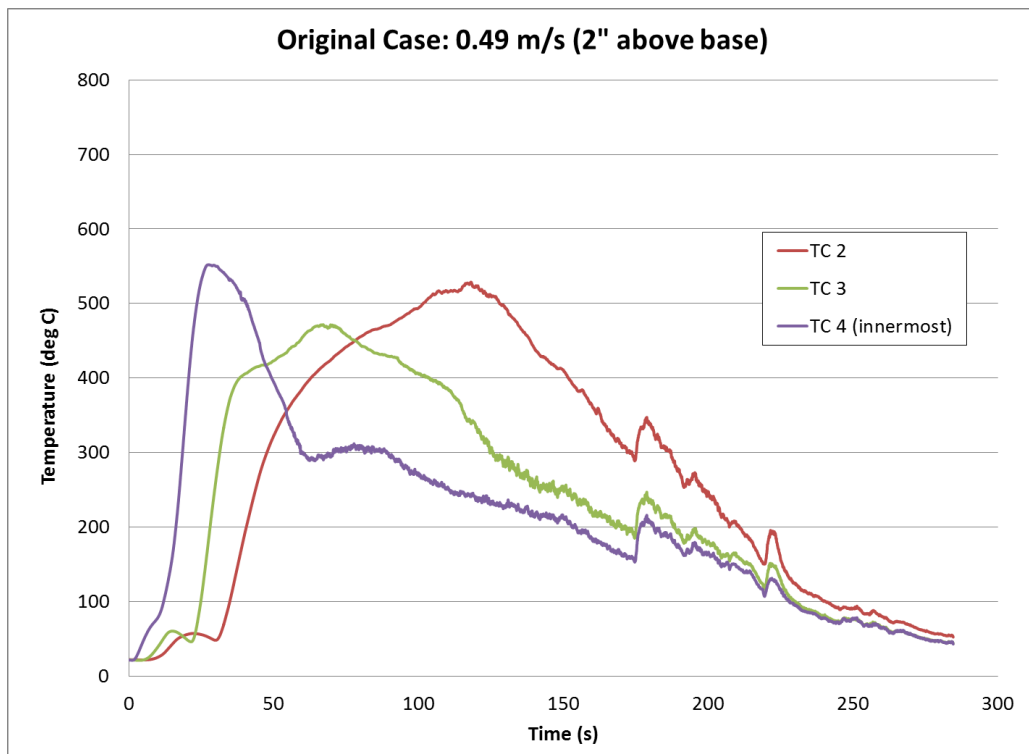


Figure C-4. Original Case: 0.49 m/s.

Appendix D: Smaller Diameter Cases

Note: Some of the thermocouples were not calibrated correctly and the resulting erroneous data are omitted.

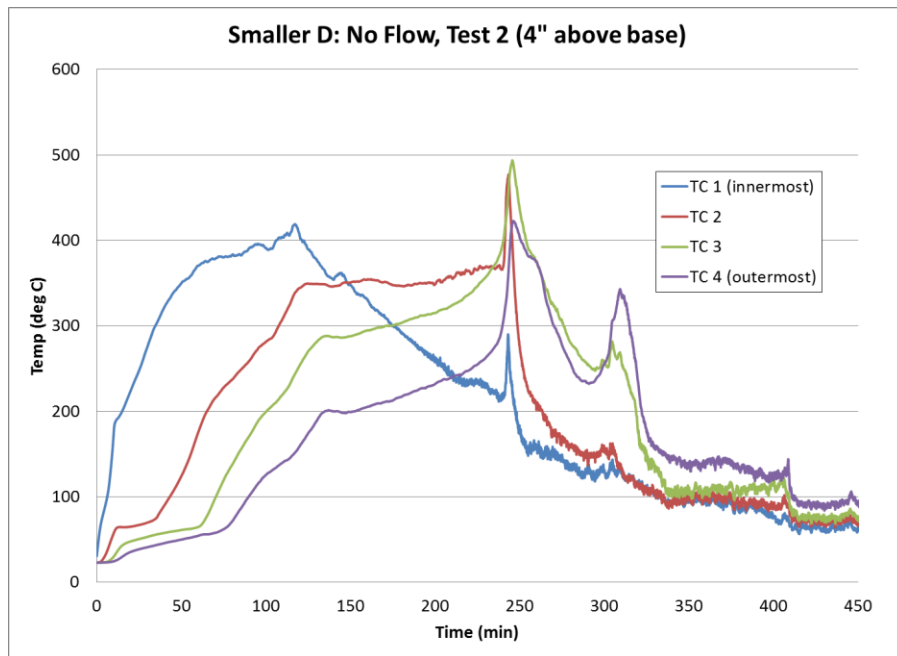


Figure D-1. Smaller diameter case: No Flow, Test 2.

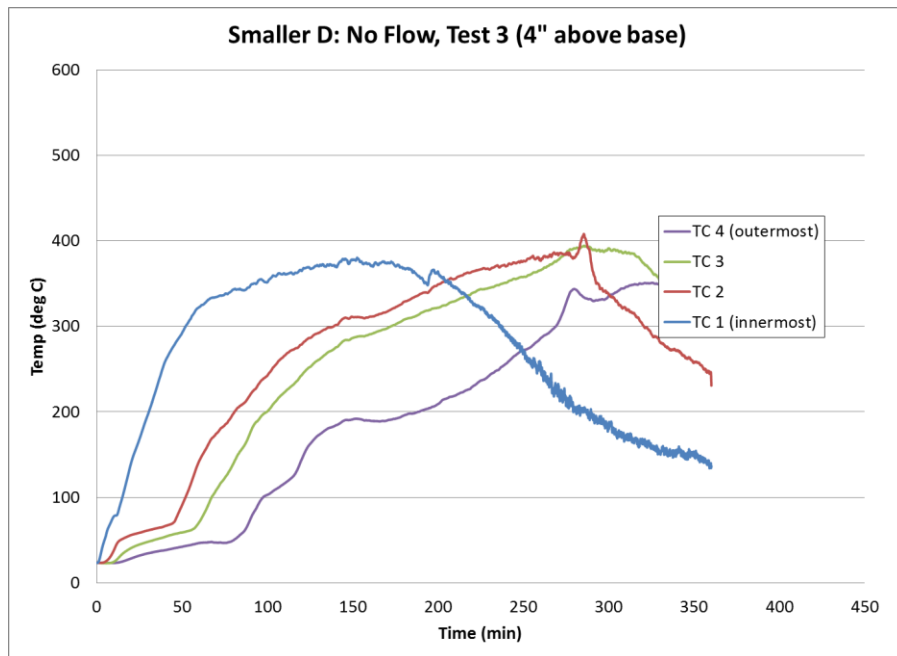


Figure D-2. Smaller diameter case: No Flow, Test 3.

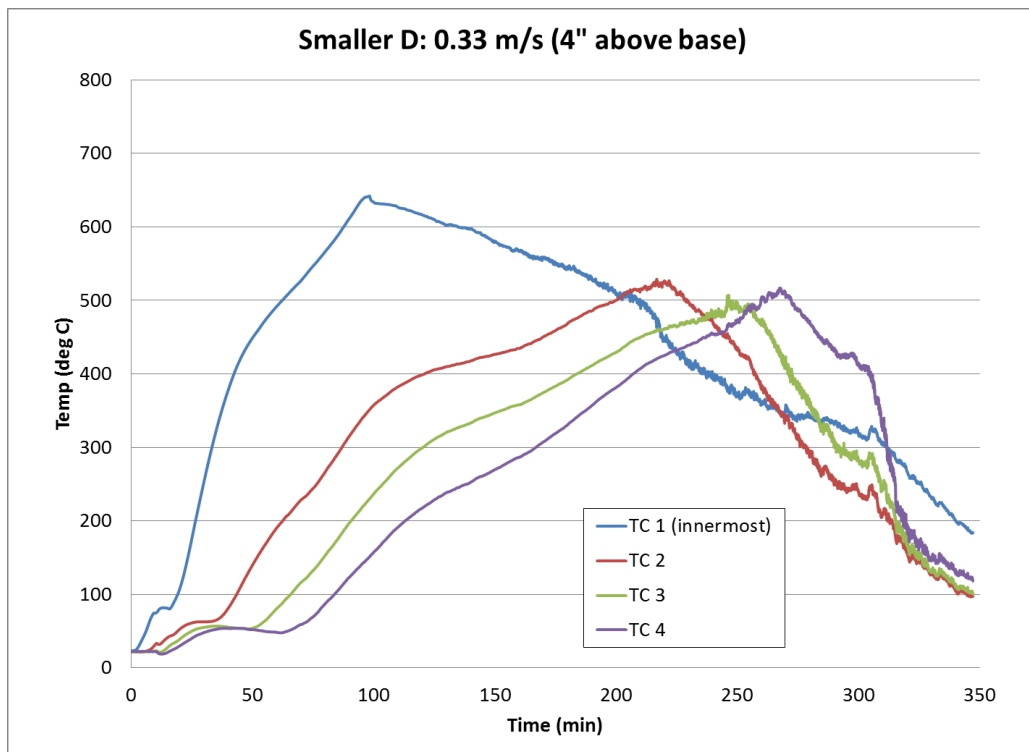


Figure D-3. Smaller diameter case: 0.33 m/s.

Appendix E: Base Case (2 and 4)

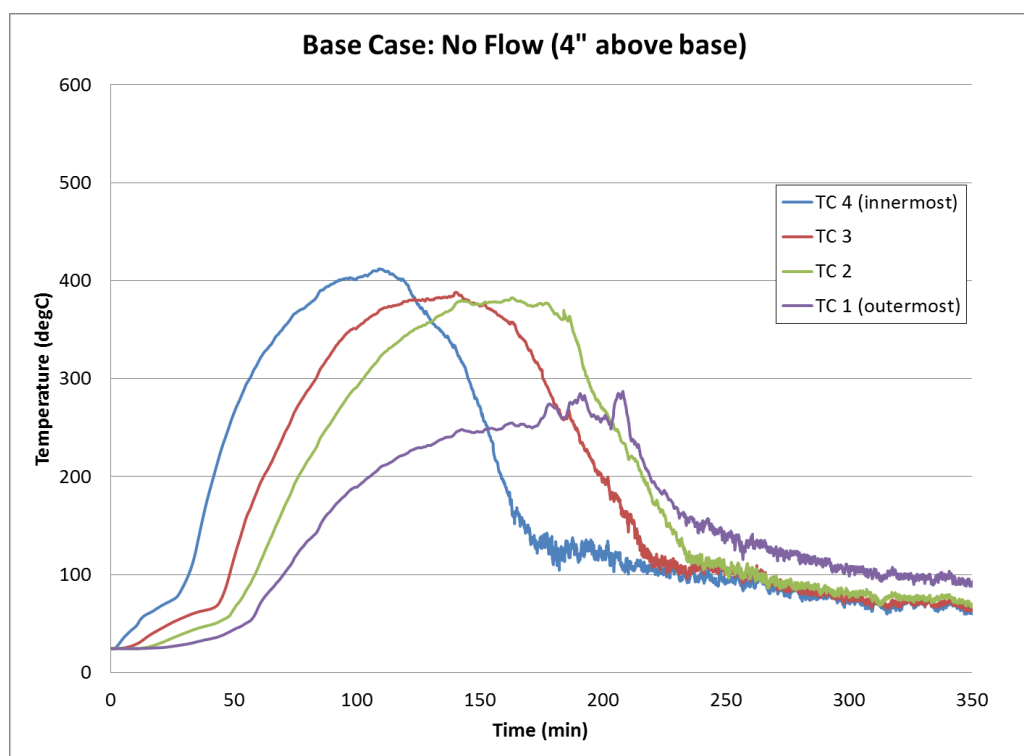


Figure E-1. Base Case: No Flow.

Appendix F: Base Case (3 and 3), without insulation

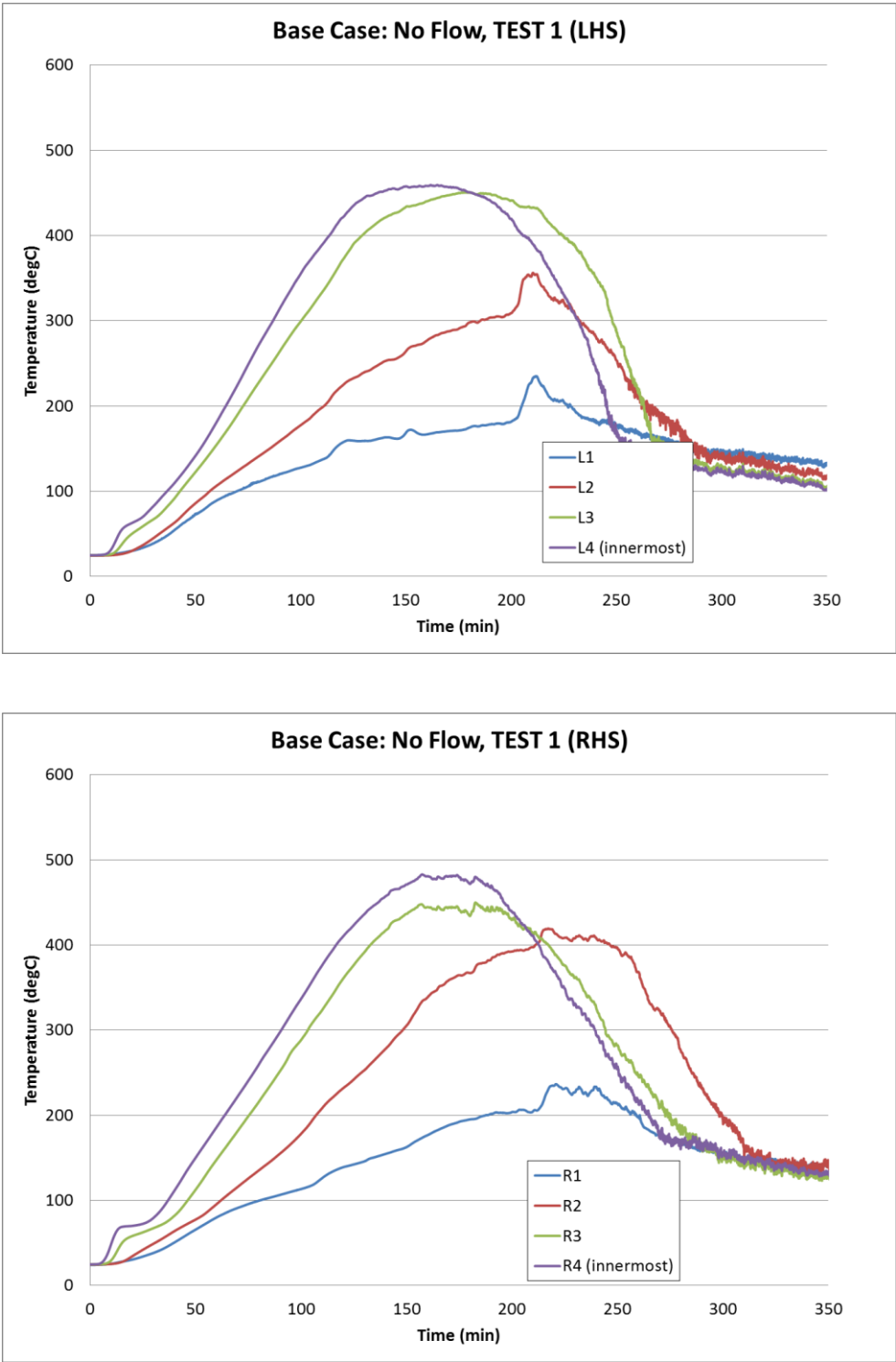


Figure F-1. Base Case: No Flow, Test 1

Appendix G: Base Case (3 and 3) with insulation

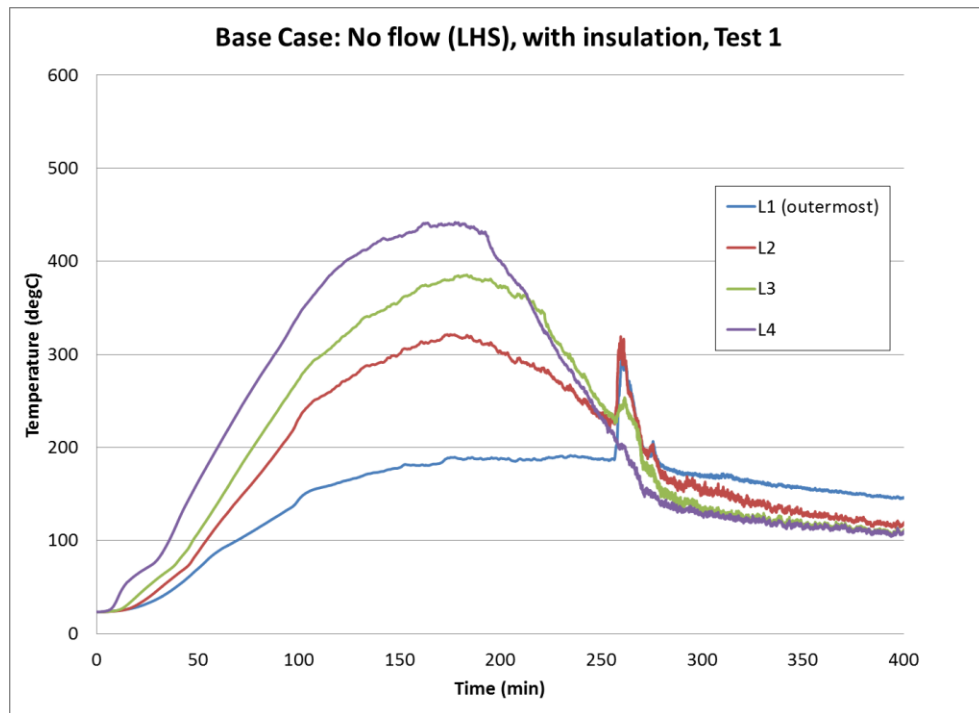
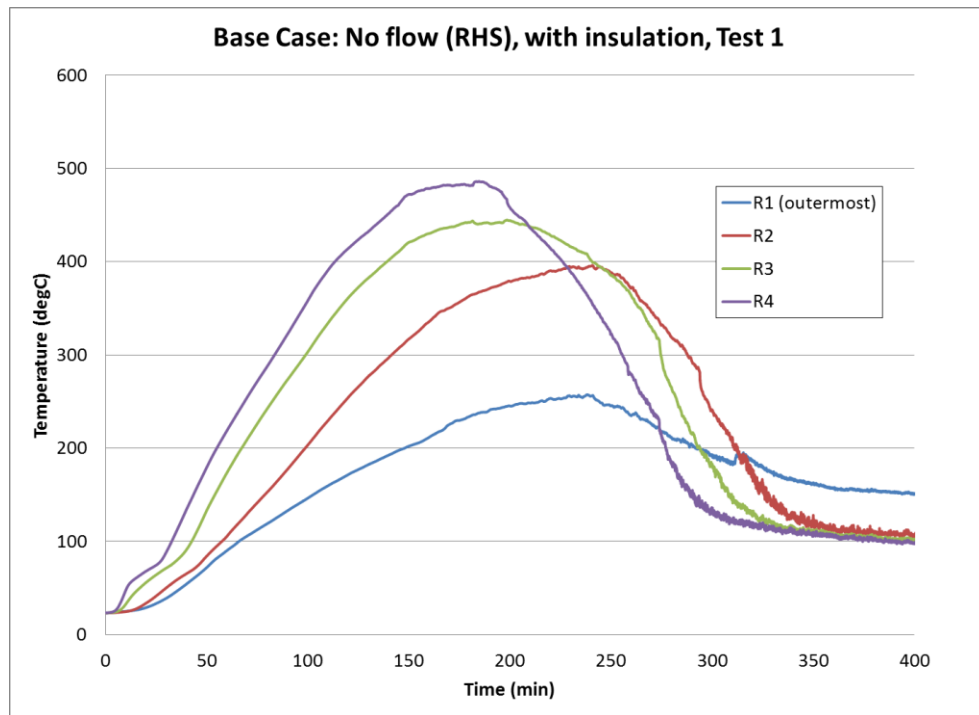


Figure G-1. Base Case: No Flow, with insulation, Test 1.

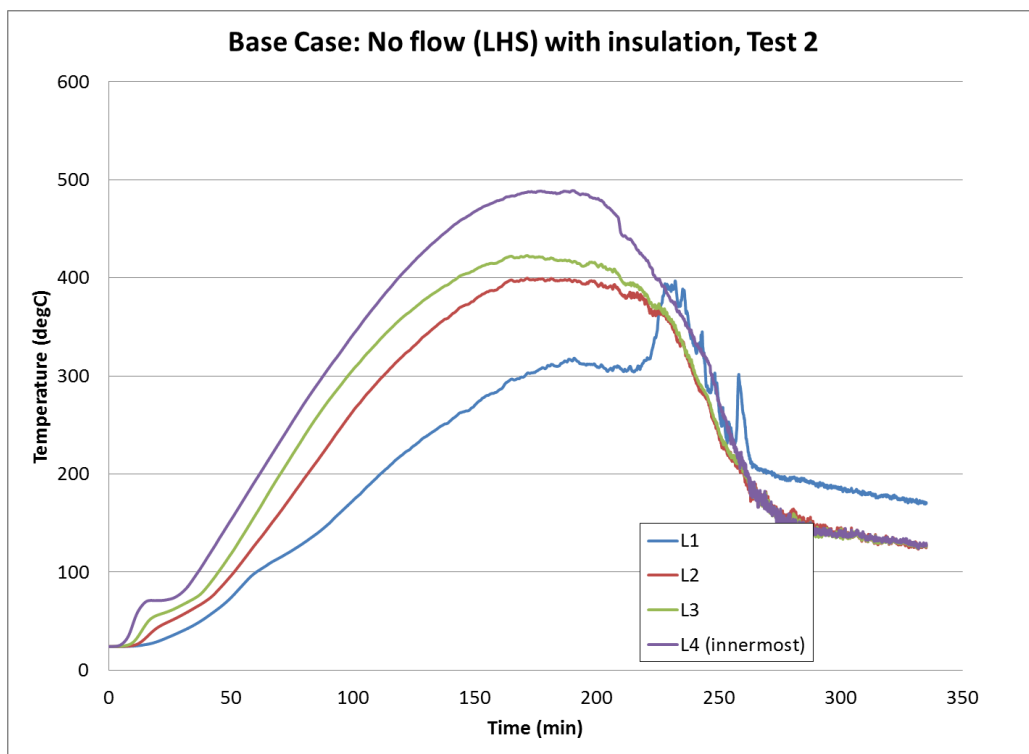
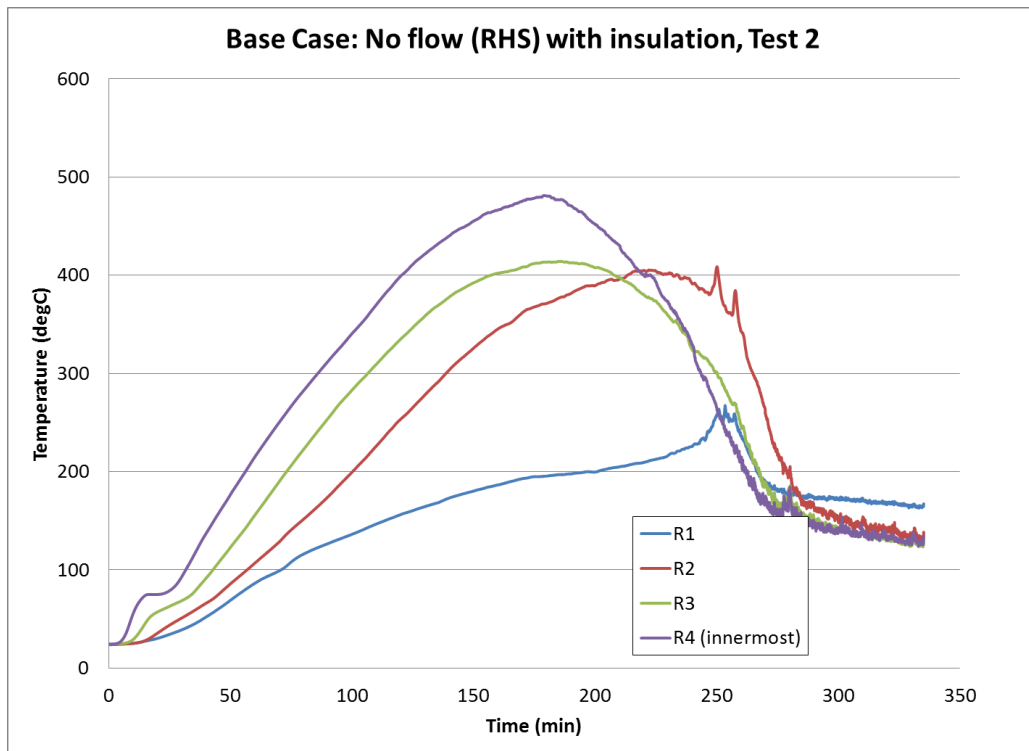


Figure G-2. Base Case: No Flow, with insulation, Test 2.

Appendix H: Air Flow Cases

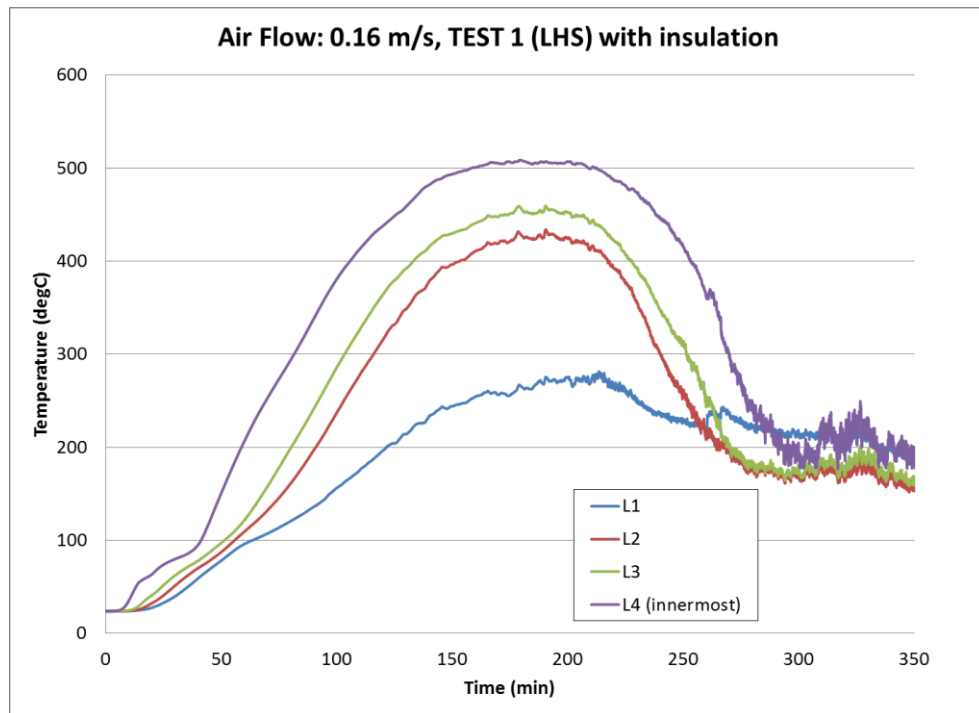
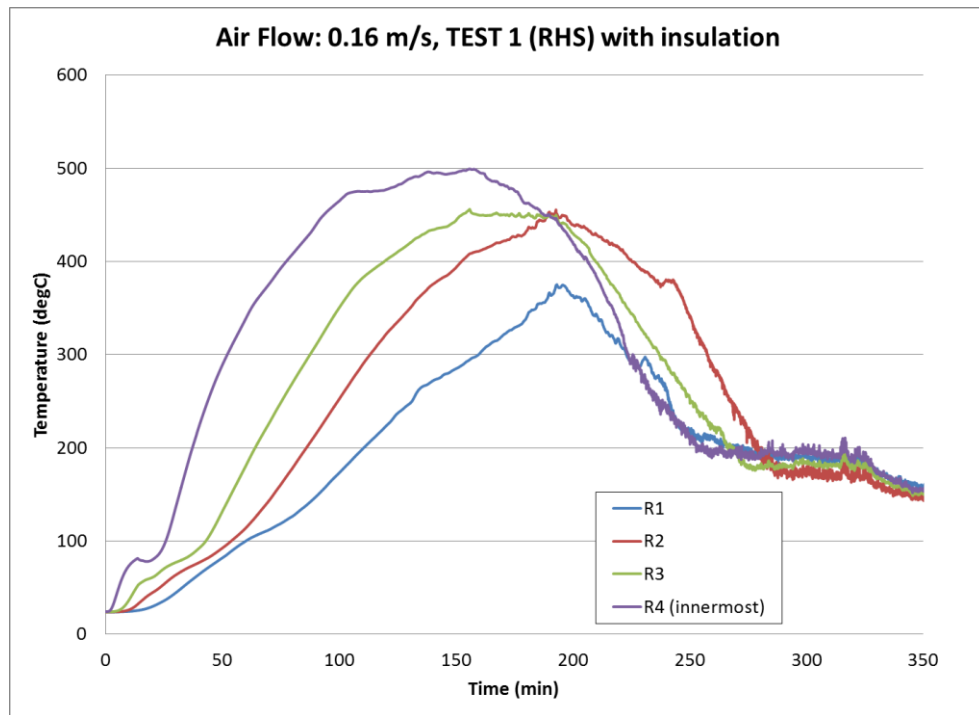


Figure H-1. Air Flow Case: 0.16 m/s, Test 1.

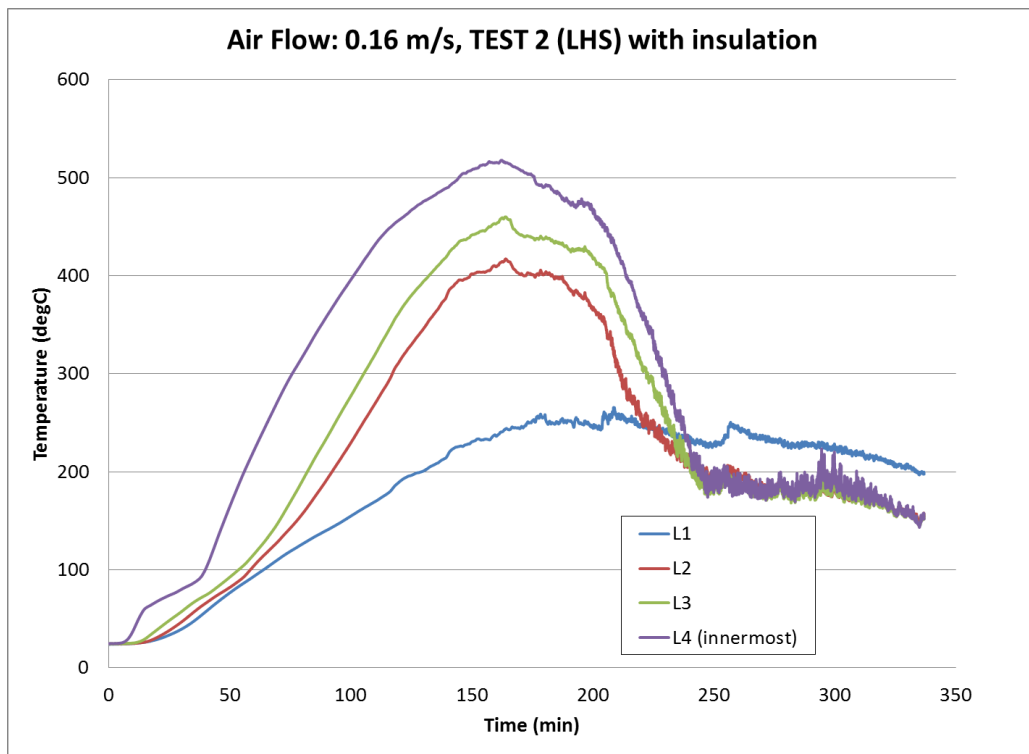
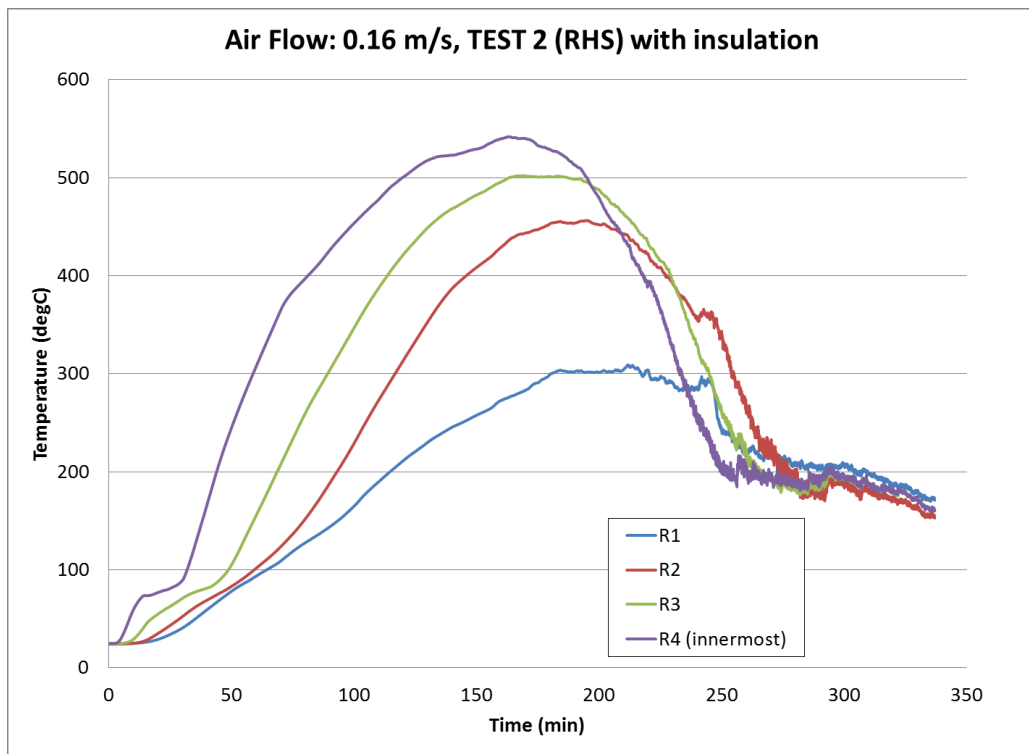


Figure H-2. Air Flow Case: 0.16 m/s, with insulation.

Appendix I: Preliminary Emission Studies

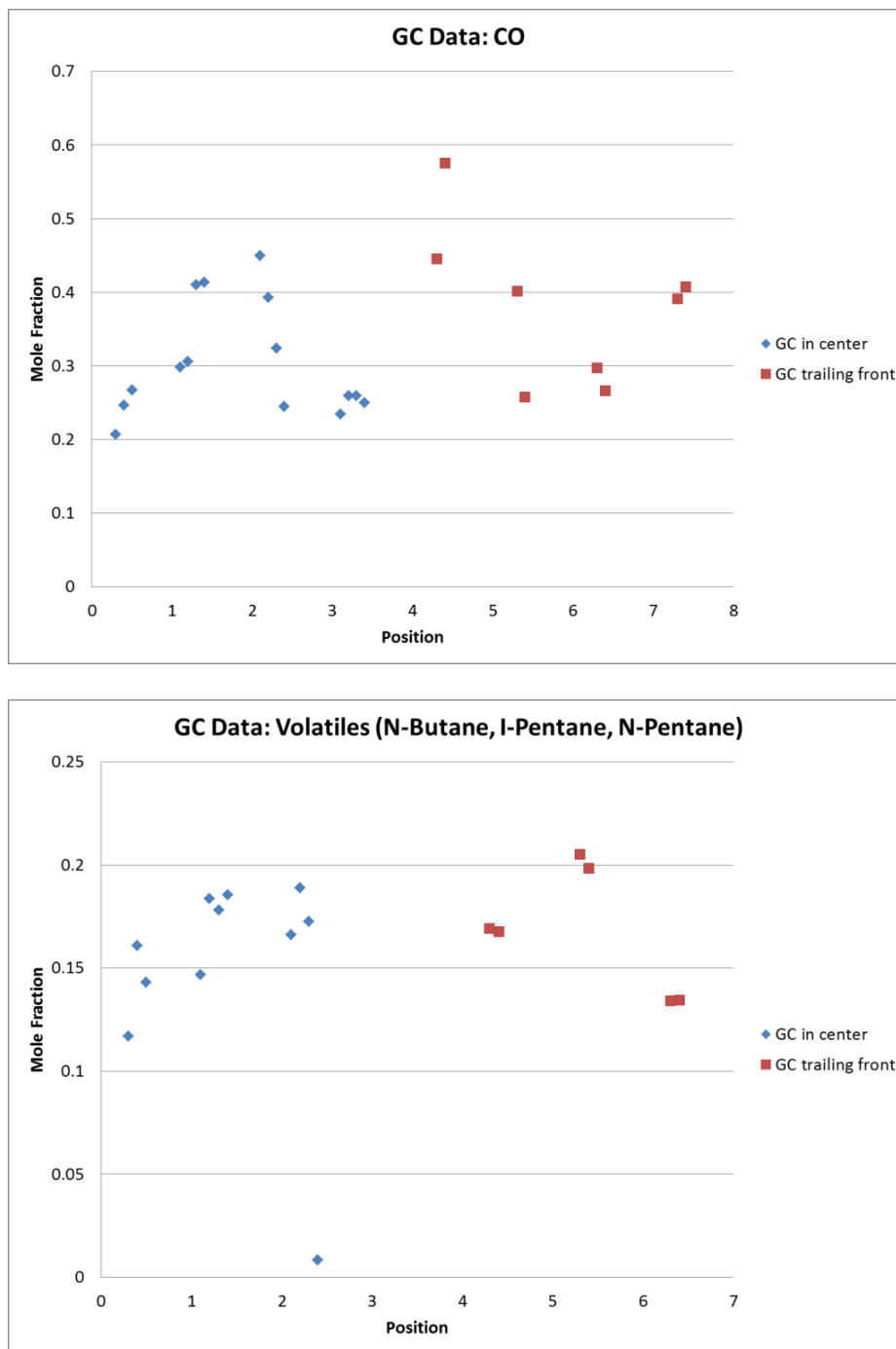


Figure I-1. GC measurements of CO and volatiles for a no air flow experiment. The GC probe is first held at various locations in the center core from axial position (0) to inner wall of the sawdust bed (3). Then the GC trails the char front all the way to the wall for positions 4 to 7.

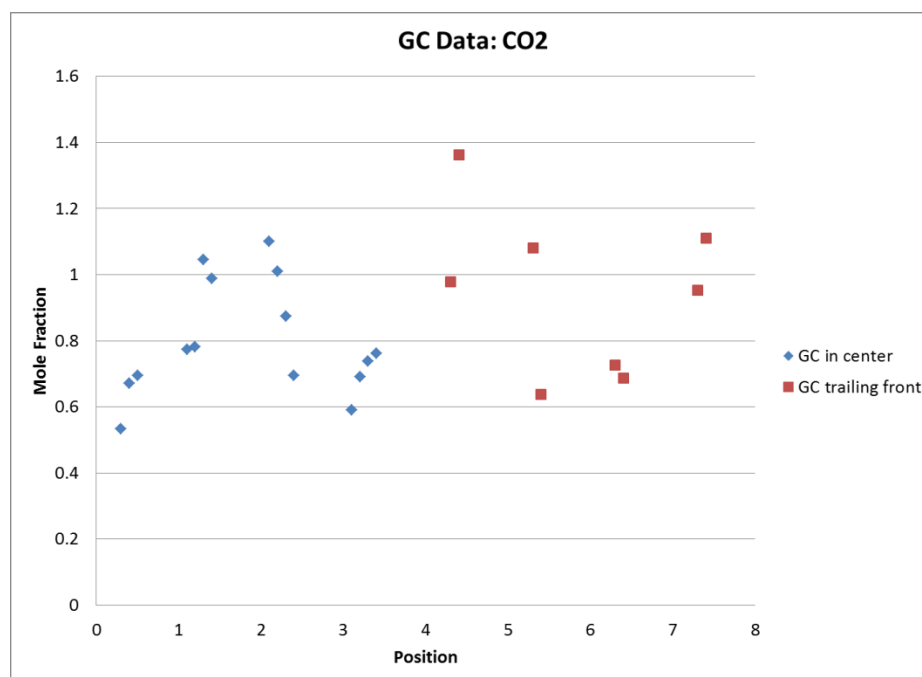


Figure I-2. GC measurement of CO₂ concentration in the exhaust. Same experimental condition as Figure I-1.

References

1. Heltberg, Rasmus. "Household Fuel and Energy Use in Developing Countries – A Multicountry Study." *Oil and Gas Policy Division*. The World Bank, 14 May 2003. Web. 10 Apr. 2013.
2. Chronicle. "Ghana Has the Highest Rate of Deforestation." *General News*. Ghana Web, 1 July 2011. Web. 11 Apr. 2013.
3. Nyarko, Ofori. "Woodfuels Use in Ghana: Social, Economic and Energy Dimensions." *Forest Energy Forum No 9*. Food and Agricultural Organization (FAO) of the United Nation, n.d. Web. 8 Apr. 2013.
4. Zhou, Zheng, Kathie L. Dionisio, and Raphael E. Arku. "Household and Community Poverty, Biomass Use, and Air Pollution in Accra, Ghana." *PNAS* 108.27 (2011): n. pag. PDF file.
5. Shafizadeh, Fred, and Allan G. W. Bradbury. "Smoldering Combustion of Cellulosic Materials." *Journal of Building Physics* 141.2 (1979): n. pag. PDF file.
6. Ohlemiller, T. J. "Modeling of Smoldering Combustion Propagation." *Progress in Energy and Combustion Science* 11.4 (1985): 270-310. Print.
7. Dahlman, Jason, and Charlie Forst. *SAWDUST COOKSTOVE*. *ECHO Appropriate Technology Note*. ECHO Community, 2001. Web. 22 Apr. 2013.
8. Manyo-Plange, Ngozi C. *The changing climate of household energy: Determinants of cooking fuel choice in domestic settings in Axim, Ghana*. SSRN, 2011. PDF file.

9. Gupta, S., et al. "EMISSION FACTORS AND THERMAL EFFICIENCIES OF COOKING BIOFUELS FROM FIVE COUNTRIES." *Biomass and Bioenergy* 14.5 (1998): 547-59. Print.
10. Leach, S. V., et al. "Kinetic and Fuel Property Effects on Forward Smoldering Combustion." *Combustion and Flame* 120.3 (2000): 346-58. Print.
11. Ohlemiller, T. J., "Smoldering Combustion." *Handbook of Fire Protection Engineering*. Ed. P. J. DiNenno et al. 3rd ed. N.p.: NIST, 2002. 200-10. Print.
12. - - -. "Smoldering Combustion Propagation on Solid Wood." *Fire Safety Science - Third International Symposium*: 565-74. Print.
13. Browder, Tommy. "Modeling Biomass Briquette Smoldering." MS thesis. U of Texas at Austin, 2010. Print.
14. Faucett, Aimie. "Exploration of Sustainable Biomass Fuels for use in the Ghanaian Gyapa Cookstove." MS thesis. U of Texas at Austin, 2010. Print.